

---

# Training-Free Bias Mitigation by LLM-Assisted Bias Detection and Latent Variable Guidance

---

**Jinya Sakurai**

The University of Tokyo  
sakurai-jinya725@g.ecc.u-tokyo.ac.jp

**Issei Sato**

The University of Tokyo  
sato@g.ecc.u-tokyo.ac.jp

## Abstract

Text-to-image (T2I) models have revolutionized content creation, empowering applications from artistic expression to education and marketing. However, their dependence on large uncensored datasets often perpetuates societal biases and raises serious ethical concerns. We introduce FairT2I, a novel training-free framework that uses large language models (LLMs) to detect and correct these biases during generation. FairT2I has three key components (1) latent variable guidance which decomposes the generative score function into a weighted sum of scores conditioned on individual latent attributes, (2) LLM based bias detection which analyzes text prompts to identify potential societal biases, and (3) attribute re-sampling which rebalances the model’s latent attributes and integrates them into input text prompts to mitigate detected biases. Unlike prior approaches, FairT2I requires no model finetuning, hyperparameter searches, or predefinition of bias categories. Our experiments, using both a uniform distribution and real-world employment statistics, show that FairT2I outperforms existing training-free bias mitigation methods. Furthermore, on the Parti Prompts dataset, FairT2I enhances image diversity without sacrificing quality or prompt fidelity, offering a better trade-off compared to classifier-free guidance.

## 1 Introduction

The rapid evolution of Text-to-image (T2I) models, exemplified by systems like Stable Diffusion [Esser et al., 2024, Podell et al., 2023], Imagen [Imagen-Team-Google et al., 2024], Flux [Black Forest Labs, 2024], has democratized content creation, allowing users to generate high-quality visuals with minimal technical expertise. However, a critical challenge persists: these models inherit and often amplify the societal biases present in their large-scale web training data [Bavalatti et al., 2025, Naik and Nushi, 2023]. The risk of T2I model generating content that reflects stereotypes and perpetuates societal inequalities is a significant ethical concern [Wan et al., 2024, Mandal et al., 2024, Sandoval-Martin and Martínez-Sanzo, 2024], further exacerbated by the trend of recycling synthetic texts and images for training, which can lead to iterative bias amplification [Wyllie et al., 2024, Alemohammad et al., 2023].

Addressing these biases effectively is critical; however, existing debiasing strategies suffer from significant drawbacks. Comprehensive data curation is inherently hard to scale [Bianchi et al., 2023]. Furthermore, many state-of-the-art techniques [Kim et al., 2024, Zhang et al., 2023, Hirota et al., 2024] demand computationally expensive model fine-tuning or retraining for each targeted bias, often coupled with onerous hyperparameter searches [Friedrich et al., 2023]. In addition, these approaches typically depend on static, predefined lists of sensitive attributes [Kim et al., 2024, Zhang et al., 2023, Hirota et al., 2024, Friedrich et al., 2023], which constrains their ability to address newly emerging biases or to adapt to evolving societal norms and contexts.

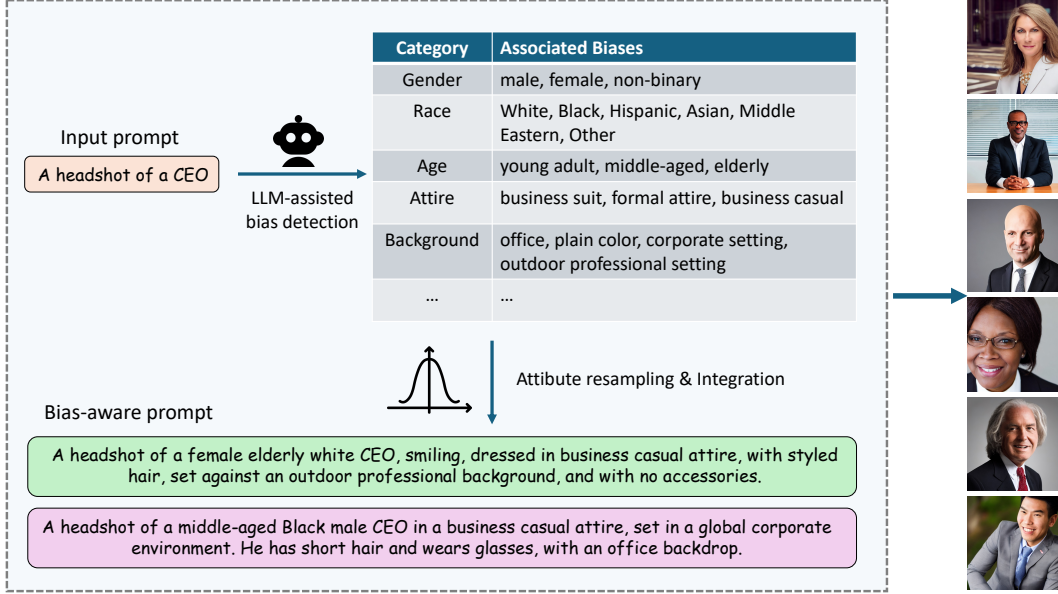


Figure 1: An overview of FairT2I. LLM detects biases latent in the input prompt and converts it into a bias aware prompt by sampling the detected attributes from fair distributions. FairT2I can be used not only for societal bias mitigation but also to improve diversity.

To address these challenges, we propose FairT2I, an effective and flexible debiasing framework for T2I models. FairT2I consists of three key components:

1. **Latent variable guidance:** We prove that the image generation process can be decomposed into (a) sampling latent biases and (b) generating images conditioned on the input text and those latent biases. We then debias the model by replacing the original T2I model’s biased latent-variable distribution (a) with a fair distribution (Section 3.2).
2. **LLM-assisted dynamic bias detection:** We use large language models to detect potential societal biases in input prompts instead of relying on fixed attribute lists (Section 3.3).
3. **Probabilistic attribute resampling:** Once biases are detected, we employ systematic resampling (e.g., uniform sampling) to adjust latent attribute distributions and steer the T2I model toward producing more varied and fair outputs (Section 3.4). The sampled attributes are seamlessly integrated into the prompt by the LLM, enabling fairer image generation.

Crucially, FairT2I operates entirely during inference, requiring no model fine-tuning, no complex hyperparameter search, and no predefined attribute lists. This makes our approach highly adaptable, computationally efficient, and readily applicable to diverse models and types of societal biases.

In experiments on the Stable Debias Profession Dataset [Luccioni et al., 2023], we demonstrate that FairT2I reduces societal bias more effectively than existing models. We verify debiasing under two types of fair attribute distributions: uniform distributions, in which all attributes appear with equal probability, and realistic distributions matching actual employment statistics. Furthermore, experiments on the Parti Prompts dataset [Yu et al., 2022] demonstrate that, beyond societal bias mitigation, FairT2I enhances output diversity while preserving high image quality (Section 5).

## 2 Related Work

**Text-to-image (T2I) models.** The generative capabilities of T2I models [Imagen-Team-Google et al., 2024, Esser et al., 2024, Chen et al., 2025a, Black Forest Labs, 2024] have improved dramatically through several key developments: training on large scale text image pairs [Schuhmann et al., 2022, Chen et al., 2023], architectural improvements [Peebles and Xie, 2023] from UNet [Ronneberger et al., 2015] to transformer based designs [Vaswani et al., 2017, Dosovitskiy et al., 2020], and theoretical developments from diffusion models [Sohl-Dickstein et al., 2015, Ho et al., 2020, Song et al., 2020]

to flow matching [Lipman et al., 2022, Liu et al., 2022, Lipman et al., 2024]. Furthermore, recent fine tuning approaches have significantly reduced generation time by minimizing the required number of inference steps [Liu et al., 2023, Chen et al., 2024a, Sauer et al., 2024, 2023, Yang et al., 2023]. A distinctive characteristic of state of the art models is their use of separately trained components, such as Variational Auto Encoders [Kingma et al., 2014] for image compression, text encoders [Raffel et al., 2020, Radford et al., 2021], and flow model backbones, each trained on different datasets.

**Societal bias in T2I models.** Numerous studies have investigated biases in T2I models. Research such as Ghosh and Caliskan [2023], Wu et al. [2023], Bianchi et al. [2023] highlights the biases embedded in generated outputs for seemingly neutral input prompts that lack explicit identity- or demographic-related terms. Other works, including Cho et al. [2022], Luccioni et al. [2023] predefine sensitive human attributes and analyze biases in outputs generated from occupational input prompts. Naik and Nushi [2023] provides broader analyses, including comparative studies with statistical data or image search results, as well as spatial analyses of generated images. Wang et al. [2023] applies methods from social psychology to explore implicit and complex biases related to race and gender. Furthermore, Luccioni et al. [2023] introduces an interactive bias analysis tool leveraging clustering methods. Lastly, Chen et al. [2024b] examines the potential for AI-generated images to perpetuate harmful feedback loops, amplifying biases in AI systems when used as training data for future models. D’Incà et al. [2024], Chinchure et al. [2023] employ LLMs to detect open-ended biases in text-to-image models where users do not have to provide predefined bias attributes.

**Bias mitigation in T2I models.** One line of work focuses on making T2I models fair by fine-tuning or retraining various components, from the diffusion backbone [Kim et al., 2024] and text encoder Hirota et al. [2024] to postfix prompt embeddings Zhang et al. [2023] or additive residual image vectors Seth et al. [2023]. While effective, such retraining is both time and resource intensive and must be repeated whenever societal notions of bias evolve. By contrast, several methods eliminate societal bias only by steering generation at inference time. FairDiffusion Friedrich et al. [2023] guides sampling with randomly chosen bias attributes; [Chuang et al., 2023] removes unwanted directions from the text embedding space via calibrated projection matrices; and ENTIGEN Bansal et al. [2022] simply appends an ethical fairness postfix to the input prompt. Although these approaches require no additional training, they do depend on a predefined list of bias categories and attribute values to control for.

### 3 Methodologies

In this section, we present FairT2I, a principled framework designed to mitigate societal biases in T2I models. Our approach unfolds in three main stages: First, we develop a latent variable formulation that explicitly captures how sensitive attributes influence the image generation process. Second, we describe an LLM-assisted mechanism for identifying prompt-induced biases without relying on predefined, fixed attribute sets. Finally, we introduce an attribute resampling scheme, grounded in real-world demographic statistics, to rebalance the outputs and steer the generated distributions toward greater fairness.

#### 3.1 Preliminaries: classifier-free guidance

In diffusion models [Ho et al., 2020, Sohl-Dickstein et al., 2015] and flow matching models [Esser et al., 2024, Lipman et al., 2022], classifier-free guidance [Ho and Salimans, 2022] is a powerful tool for sampling images  $\mathbf{x}$  conditioned on a text input  $\mathbf{y}$ . It accomplishes this by guiding an unconditional image generation model using the score function  $\nabla_{\mathbf{x}} \log p(\mathbf{x})$ . This enables the sampling from

$$p_w(\mathbf{x}, \mathbf{y}) \propto p(\mathbf{x})p(\mathbf{y} | \mathbf{x})^w \propto p(\mathbf{x})^{1-w}p(\mathbf{x} | \mathbf{y})^w$$

where  $w \in \mathbb{R}$  is the guidance scale typically used with  $w > 1$ . The score satisfies

$$\nabla_{\mathbf{x}} \log p_w(\mathbf{x}, \mathbf{y}) = (1 - w)\nabla_{\mathbf{x}} \log p(\mathbf{x}) + w\nabla_{\mathbf{x}} \log p(\mathbf{x} | \mathbf{y})$$

so by training the network to predict both the unconditional score  $\nabla_{\mathbf{x}} \log p(\mathbf{x})$  and conditional score  $\nabla_{\mathbf{x}} \log p(\mathbf{x} | \mathbf{y})$ , flexible sampling from the conditional distribution can be achieved through a weighted sum of the network outputs.

Whereas in classifier-free guidance, the weights for the score functions are typically set to achieve a trade-off between sample quality and text fidelity, our formulation 3 sets these weights to ensure fair image generation.

### 3.2 Latent variable guidance for bias mitigation

In latent variable guidance, societal bias is controlled by decomposing the network’s predicted score function into a weighted sum of component score functions, each conditioned on a distinct latent variable. These weights are then adjusted to enforce fairness in the generated outputs. Central to our formulation is the following proposition:

**Proposition 1.** *Let  $\mathbf{y}$  represent the input text,  $\mathbf{x}$  the generated image, and  $\mathbf{z}$  the latent attribute, and assume conditional independence between  $\mathbf{x}$  and  $\mathbf{z}$  given  $\mathbf{y}$ , the following equation holds:*

$$\nabla_{\mathbf{x}} \log p(\mathbf{x} | \mathbf{y}) = \sum_{z \in Z} p(\mathbf{z} = z | \mathbf{y}) \nabla_{\mathbf{x}} \log p(\mathbf{x} | \mathbf{z} = z, \mathbf{y}). \quad (1)$$

*Proof.* See Appendix A. □

This formulation, presented in Equation (1), effectively decomposes the score function guiding the image generation process. It explicitly separates the influence of the latent attribute  $\mathbf{z}$  (which is sampled according to its conditional probability  $p(\mathbf{z} | \mathbf{y})$ ) from the subsequent image generation step, which is guided by both this sampled attribute  $\mathbf{z}$  and the original input text  $\mathbf{y}$ . This perspective allows us to contextualize existing bias mitigation strategies. Approaches such as replacing text encoders with fair alternatives [Hirota et al., 2024, Chuang et al., 2023], learning fair prompt embeddings [Zhang et al., 2023], or randomly sampling sensitive attributes [Friedrich et al., 2023] can all be interpreted as methods that implicitly or explicitly substitute the T2I model’s original, potentially biased distribution  $p_{\text{bias}}(\mathbf{z} | \mathbf{y})$  with a more equitable target distribution  $p_{\text{fair}}(\mathbf{z} | \mathbf{y})$ .

In practice, computing the summation over all possible values of  $z$  in Equation (1) can be computationally prohibitive, especially when dealing with a large or continuous space of latent attributes. To overcome this computational challenge, we employ Monte Carlo sampling from the distribution  $p(\mathbf{z} | \mathbf{y})$ . Specifically, we approximate the expectation in Equation (1) using a finite number of samples. For the simplest case, using an approach with a single sample, this approximation becomes:

$$\nabla_{\mathbf{x}} \log p(\mathbf{x} | \mathbf{y}) \approx \nabla_{\mathbf{x}} \log p(\mathbf{x} | \tilde{\mathbf{z}}, \mathbf{y}), \text{ where } \tilde{\mathbf{z}} \sim p(\mathbf{z} | \mathbf{y}).$$

While this approach using a single sample provides an unbiased estimate of the true score, it may exhibit higher variance compared to the exact summation. This variance can be mitigated by using additional samples; however, this benefit comes at the cost of increased computation time. Consequently, a careful trade-off between computational efficiency and the accuracy of the score estimation must be considered when implementing this approach in practical scenarios.

### 3.3 LLM-assisted bias detection

To implement latent variable guidance, we need to define a candidate set of biases  $Z$ . The simplest approach is to predefine a closed set of biases such as race and gender; however, this approach has several limitations. For instance, one significant limitation relates to computational challenges. The diversity of input prompts is virtually infinite, meaning that a predefined set of latent attributes  $Z$  can only appropriately handle a limited subset of these cases. Consequently, it is practically impossible to predefine a suitable  $Z$  for every conceivable prompt in advance. Another limitation concerns incomplete representation. If the latent attribute set  $Z$  is defined manually in a rule-based manner, it may fail to fully capture the diversity and context of the real world. This approach also risks overlooking biases embedded in the input text that are beyond human recognition.

To address these challenges, we leverage large language models (LLMs) [OpenAI et al., 2024, Anthropic, 2025] to automatically detect biases in the input text, as with existing bias detection methods [D’Incà et al., 2024, Chinchure et al., 2023]. Specifically, we use the LLM to predict the set of possible latent attributes  $Z$  from the input text  $\mathbf{y}$ . LLMs are prompted to output a set of latent attributes that are likely to appear in images generated by T2I models with the input text in a JSON format. This approach allows us to handle a broader range of input prompts and to detect biases that may not be apparent to human annotators.



### 3.4 Attribute resampling

When we have a set of latent attributes  $Z$  from LLM as potential biases in the input prompts, we can formulate  $p_{\text{fair}}(\mathbf{z} = z \mid \mathbf{y})$  to perform sampling that mitigates bias. We consider two approaches to defining  $p_{\text{fair}}(\mathbf{z} = z \mid \mathbf{y})$ .

**Uniform distribution.** One simple approach is to set the distribution of latent attributes to be uniform across all possible values of  $z$ :  $p_{\text{fair}}(\mathbf{z} = z \mid \mathbf{y}) = \frac{1}{|Z|}$ , which corresponds to simply mixing the scores  $\nabla_{\mathbf{x}} \log p(\mathbf{x} \mid \mathbf{z} = z, \mathbf{y})$  with equal proportions across all possible values of  $z$ . This formulation coincides with that of Fair Diffusion [Friedrich et al., 2023].

**Employment statistics.** Research has shown that T2I models tend to exaggerate demographic stereotypes beyond what we observe in real-world distributions across various latent attributes [Naik and Nushi, 2023]. One way to address this issue is to incorporate real-world statistical data as  $p_{\text{fair}}(\mathbf{z} = z \mid \mathbf{y})$ , ensuring that the generated image distributions are at least as balanced as real-world demographics.<sup>1</sup>

Upon sampling the latent attribute  $z$  from the fair conditional distribution  $p_{\text{fair}}(\mathbf{z} = z \mid \mathbf{y})$ , we need to compute the score  $\nabla_{\mathbf{x}} \log p(\mathbf{x} \mid \mathbf{z} = z, \mathbf{y})$ . To enforce that the T2I model incorporates the sampled attribute  $z$ , we use an LLM to naturally fuse the textual input  $\mathbf{y}$  and the latent attribute  $\mathbf{z}$ , and feed this augmented text  $\mathbf{y} \oplus \mathbf{z}$  directly into the T2I model in place of  $\mathbf{y}$ .

## 4 Experiments: Societal Bias Mitigation

In this section, we present comparative experiments against existing methods to demonstrate that FairT2I can detect diverse biases in input text and generate images that effectively mitigate them.

### 4.1 Experimental settings

**Evaluation dataset.** To evaluate societal bias regarding professions, we use the occupation dataset from Stable Bias [Luccioni et al., 2023] (hereafter referred to as the Stable Bias profession dataset), which contains 131 occupations sourced from the U.S. Bureau of Labor Statistics (BLS) (see Appendix A of Luccioni et al. [2023] for full dataset details). We consider two target distributions: (1) the uniform distribution over categories defined in FairFace [Karkkainen and Joo, 2021], and (2) BLS occupational statistics. For the uniform distribution, we randomly sampled a subset of 50 occupations from this dataset. For the BLS statistics, we use the five occupation prompts mentioned in Naik and Nushi [2023]: *CEO*, *doctor*, *computer programmer*, *nurse*, and *house keeper*. As with Zhang et al. [2023] each profession is prefixed with “A headshot of ” to form an input prompt. Details of this subset are provided in Appendix B.1.

**Evaluation metrics.** Following Hirota et al. [2024], Chuang et al. [2023], we measure bias in the generated outputs by computing the statistical parity [Choi et al., 2020] between the empirical distribution and the target ideal distribution. In line with Naik and Nushi [2023], we detect faces in the generated images using dlib [King, 2015] and then predict each image’s attributes using classifiers trained on the FairFace dataset [Karkkainen and Joo, 2021]. Statistical parity is defined as the  $\ell_2$ -distance between two probability vectors. Specifically, let  $\mathbf{p} = (p_1, p_2, \dots, p_n)$ ,  $\mathbf{q} = (q_1, q_2, \dots, q_n)$  be two distributions over  $n$  outcomes. Then the statistical parity between  $\mathbf{p}$  and  $\mathbf{q}$  is

$$\text{SP}(\mathbf{p}, \mathbf{q}) = \|\mathbf{p} - \mathbf{q}\|_2 = \sqrt{\sum_{i=1}^n (p_i - q_i)^2}.$$

A lower statistical parity indicates that the distribution of generated images more closely matches the target (fair) distribution.

For each prompt in our subset, we generate 200 images, classify each by its FairFace attribute, and compute statistical parity. Further details appear in Appendix B.2.

<sup>1</sup>It is worth noting that real-world occupational distributions often reflect systemic biases and unequal access to opportunities, shaped by historical and societal factors such as limited access to education or workplace discrimination. These disparities highlight that real-world distributions are not inherently fair.

Table 1: Biased attributes associated with the input text “*a headshot of a psychologist*” as generated by LLM.

| Attribute Category | Associated Biases  |
|--------------------|--|
| Gender             | male, female, non-binary   |
| Race               | White, Black, Asian, Hispanic, Middle Eastern, Other                         |
| Age                | young adult, middle-aged, elderly  |
| Attire             | formal business attire, casual professional, white coat, sweater with blazer |
| Accessories        | glasses, no glasses, jewelry, no jewelry                                     |
| Facial Hair        | beard, mustache, clean-shaven  |
| Hair Style         | short, long, balding, styled, natural  |
| Setting            | office, bookshelf background, plain background, clinical setting             |
| Expression         | serious, smiling, attentive, compassionate                                   |



Figure 2: Generated images for the input text “*a headshot of a psychologist*” by the original Stable Diffusion, ENTIGEN, FairDiffusion, and FairT2I (Ours).

**Methods for comparison.** We compare FairT2I against existing debiasing methods that don’t require any model finetuning:

- **Original:** the unmodified Stable Diffusion model [Rombach et al., 2022a], with no bias mitigation.
- **ENTIGEN** [Bansal et al., 2022]: appending an ethical injection phrase to the end of the prompt.
- **Fair Diffusion** [Friedrich et al., 2023]: randomly sampling attributes from a predefined bias set and applying semantic guidance [Brack et al., 2023].

Detailed hyperparameter settings for each method are provided in Appendix B.3 and B.4, respectively. To ensure a fair comparison, the T2I model was standardized to Stable Diffusion 1.5 [Rombach et al., 2022b] across all baseline and proposed methods.

**Implementation details.** We utilized Stable Diffusion 1.5 [Rombach et al., 2022b] as our T2I model. This choice was made because the hyperparameter settings and text encoders of the comparison methods were not compatible with the latest T2I architectures [Esser et al., 2024]. We employed Claude 3.7-sonnet [Anthropic, 2025] for LLM-assisted bias detection, and GPT4o-mini [OpenAI et al., 2024] to fuse the textual input  $y$  with the sensitive attribute  $z$ . Parameter settings for image generation and the exact prompts supplied to the LLM are detailed in Appendix B.5.

## 4.2 Results

**Targeting uniform distribution.** Table 2 reports the SP scores comparing empirical and uniform distributions of gender and race in the Stable Bias Profession subset. FairT2I most closely matches the uniform baseline on both metrics. Figure 3 visualizes these results alongside the ideal uniform distribution as the stacked bar charts. Together, they demonstrate that, compared to existing methods, FairT2I generates data for each attribute with greater uniformity.

Table 1 summarizes the attribute categories (race, gender, age, background, pose, and more) and the biases detected by the LLM for the prompt “*a headshot of a psychologist*”. Figure 2 then presents randomly selected outputs from each method. While the baseline methods reproduce skewed or ho-

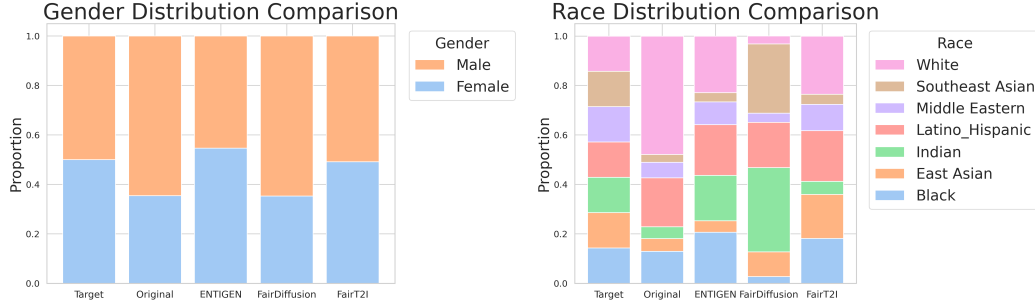


Figure 3: Comparison of the target uniform distribution and empirical distributions produced by original Stable Diffusion, ENTIGEN, FairDiffusion and FairT2I (Ours) for gender (left) and race (right), shown as stacked bar charts.

Table 3: Gender Statistical Parity (top) and Race Statistical Parity (bottom) scores (lower is better) between BLS statistics for CEO, computer programmer, doctor, nurse and housekeeper in images from the original Stable Diffusion, ENTIGEN, FairDiffusion and FairT2I (Ours). For each metric and occupation, the best score is shown in bold.

| Method                                 | Gender SP ↓   |               |               |               |               |
|--|---------------|---------------|---------------|---------------|---------------|
|  | CEO           | comp. prog.   | doctor        | nurse         | housekeeper   |
| Original                               | 0.3637        | 0.1651        | 0.3843        | 0.1796        | 0.1459        |
| ENTIGEN [Bansal et al., 2022]          | 0.3748        | 0.0569        | 0.1229        | 0.1210        | <b>0.0121</b> |
| FairDiffusion [Friedrich et al., 2023] | 0.1956        | 0.1089        | 0.1138        | 0.1653        | 0.1597        |
| FairT2I (Ours)                         | <b>0.0710</b> | <b>0.0170</b> | <b>0.0550</b> | <b>0.0537</b> | <b>0.0121</b> |

| Method                                 | Race SP ↓     |               |               |               |               |
|--|---------------|---------------|---------------|---------------|---------------|
|  | CEO           | comp. prog.   | doctor        | nurse         | housekeeper   |
| Original                               | 0.6050        | 0.2213        | 0.2110        | 0.1971        | 1.0207        |
| ENTIGEN [Bansal et al., 2022]          | 0.5004        | 0.6115        | 0.4727        | 0.4805        | 0.9341        |
| FairDiffusion [Friedrich et al., 2023] | 0.1664        | 0.1484        | <b>0.0750</b> | <b>0.1285</b> | 0.3074        |
| FairT2I (Ours)                         | <b>0.0677</b> | <b>0.0885</b> | 0.1137        | 0.1541        | <b>0.2001</b> |

homogeneous attribute distributions, FairT2I addresses the biases listed in Table 1, yielding high-quality headshots with balanced diversity across race, gender, accessories (e.g., glasses), and backgrounds.

**Targeting BLS statistics.** Table 3 summarizes the gender and race SP scores between BLS statistics for *CEO*, *computer programmer*, *doctor*, *nurse*, and *housekeeper* prompts across four methods. FairT2I consistently achieves the lowest gender SP, outperforming ENTIGEN and FairDiffusion by large margins. For race SP, FairT2I yields the best scores on *CEO*, *computer programmer*, and *housekeeper*. These results confirm that FairT2I can also steer the generated distributions toward specified target distributions. See Appendix B.8 for bar-chart comparisons and further details.

Table 2: Statistical Parity of Gender and Race Distributions by the original Stable Diffusion, ENTIGEN, FairDiffusion, and FairT2I (Ours).

| Method        | Gender SP ↓   | Race SP ↓     |
|---------------|---------------|---------------|
| Original      | 0.2056        | 0.3907        |
| ENTIGEN       | 0.0661        | 0.2001        |
| FairDiffusion | 0.2083        | 0.3137        |
| FairT2I       | <b>0.0123</b> | <b>0.1864</b> |

## 5 Experiments: Diversity Control

In this section, we evaluate FairT2I not only for its ability to mitigate societal bias but also for its capacity to enhance the diversity of generated images. To this end, we measure diversity on a more

Table 4: Comparison of classifier-free guidance (CFG) at guidance scales 7.0, 4.0, and 1.0 and of FairT2I on the FID, CLIPScore, CLIP Trace, and BLIP2 Trace metrics. A guidance scale of 1.0 corresponds to generation without CFG.

| Method           | FID ↓ | CLIPScore ↑ | CLIP Trace ↑ | BLIP2 Trace ↑ |
|------------------|-------|-------------|--------------|---------------|
| CFG-7.0          | 27.13 | 29.84       | 11.66        | 247.01        |
| CFG-4.0          | 26.46 | 30.09       | 11.87        | 250.24        |
| No CFG (CFG-1.0) | 34.47 | 28.06       | 21.05        | 473.64        |
| FairT2I (Ours)   | 26.24 | 28.35       | 19.18        | 454.49        |

general prompt dataset, demonstrating that FairT2I can improve variability of outputs beyond societal bias control.

## 5.1 Experimental settings

**Evaluation dataset.** We employ the Parti Prompt dataset [Yu et al., 2022], which comprises over 1,600 diverse English prompts intended to rigorously evaluate T2I generation models and probe their limitations. In this work, we focus on the uniform prompt distribution, as no particular target distribution is assumed. For practical efficiency, we randomly sample 50 prompts from the full dataset. The selected subset of prompts is listed in Appendix C.1.

**Evaluation metrics.** To assess image fidelity, we compute the Fréchet Inception Distance (FID) [Heusel et al., 2017] on the COCO Karpathy test split [Lin et al., 2014]. To evaluate text-image alignment, we report the CLIPScore [Hessel et al., 2021] between each generated image and its input prompt. To quantify diversity, we embed all generated images into feature spaces of both CLIP [Radford et al., 2021] and BLIP2 [Li et al., 2023], compute the covariance matrix of these embeddings, and use its trace as a diversity metric. For each prompt in our subset, we generate 200 images and calculate the CLIPScore and embedding-trace accordingly.

**Methods for comparison.** We compare FairT2I against classifier-free guidance (CFG) [Ho and Salimans, 2022] applied at three different guidance scales (7.0, 4.0 and 1.0), which is known to modulate the trade-off between image fidelity and diversity.

**Implementation details.** We use Stable Diffusion 3.5-large [Esser et al., 2024] as the T2I model. We employed Claude 3.7-sonnet [Anthropic, 2025] for LLM-assisted bias detection, and GPT4o-mini [OpenAI et al., 2024] to fuse the textual input  $y$  with the sensitive attribute  $z$ . Parameter settings for image generation and the exact prompts supplied to the LLM are detailed in Appendix C.3.

## 5.2 Results

Table 4 presents quantitative evaluations in terms of FID, CLIPScore, CLIP Trace and BLIP2 Trace, illustrating the trade-off between image fidelity, text alignment and diversity. Under CFG 7.0 and CFG 4.0, FID values are low but Trace metrics remain small. By contrast, CFG 1.0 yields a high Trace value at the expense of elevated FID. Unlike these existing methods, FairT2I achieves low FID and high Trace without substantially reducing CLIPScore. Table 5 lists the attribute categories and biases detected by LLM for the prompt “an airplane flying into a cloud that looks like a monster.” in the Parti Prompts dataset. Figure 4 then presents the images generated by each method for the same prompt. While classifier-free guidance cannot achieve both image quality and diversity, FairT2I succeeds on both measures.

## 6 Limitations

**LLM bottlenecks.** As shown in Figure 3, FairT2I generates fewer images for *Southeast Asian* and *Indian* categories compared to other classes. This is because the LLM does not detect *Southeast Asian* or *Indian* as race categories. By explicitly supplying these attributes as few shot examples in the LLM prompt, this issue can be mitigated.

**Text encoder bottlenecks.** FairT2I reflects latent attributes in image generation via explicit prompt modifications. As demonstrated by Hirota et al. [2024], information such as gender that is explicitly

Table 5: Attribute categories and their associated options generated by LLM for the input text “an airplane flying into a cloud that looks like monster.”.

| Attribute Category | Associated Biases   |
|--------------------|---|
| Type of Airplane   | commercial airliner, private jet, military aircraft, propeller plane, biplane |
| Cloud Appearance   | dark and menacing, fluffy and cute, wispy and ethereal                        |
| Monster Type       | dragon-like, humanoid, tentacled creature, multi-eyed beast, fanged monster   |
| Time of Day        | daytime, sunset, night, dawn  |
| Weather Conditions | clear sky, stormy, partly cloudy  |
| Viewing Angle      | from below, from above, side view, frontal view                               |
| Artistic Style     | photorealistic, cartoonish, dramatic, whimsical, ominous                      |
| Color Palette      | bright and colorful, dark and moody, pastel, monochromatic                    |
| Sky Background     | clear blue, sunset colors, stormy gray, gradient                              |



Figure 4: Generated images for the input text “an airplane flying into a cloud that looks like monster.” by classifier-free guidance (CFG) at guidance scales 7.0, 4.0, and 1.0 and FairT2I (Ours). A guidance scale of 1.0 corresponds to generation without CFG.

specified is accurately captured by the text encoder in the generated images. However, long prompts and complex logical relations [Tang et al., 2023, Zhang et al., 2023] may not be reflected in the outputs. This limitation could potentially be addressed by using a long context model [Zhang et al., 2024] or a vision language model based text encoder [Chen et al., 2025b].

## 7 Discussions and Conclusions

In this paper, we have presented FairT2I, a novel approach to debiasing T2I models by decomposing score functions using latent variable guidance and leveraging LLMs for bias detection and attribute resampling. We confirmed FairT2I can effectively debias T2I models without the need for model fine-tuning or tedious hyper parameter tuning. Furthermore, FairT2I can be used not only for societal bias mitigation but also to improve diversity.

**Broader impact.** FairT2I promotes fairer and more diverse image generation, helping to reduce stereotypes and improve representation of marginalized groups. Nonetheless, since FairT2I can theoretically sample from any latent attribute distribution, an adversary could intentionally specify an extremely skewed distribution to generate discriminatory or inflammatory content, posing a risk of misuse for spreading misinformation or hate speech. It is essential to continuously monitor and evaluate the impact of our debiasing methods to ensure they align with evolving social norms and ethical standards.

## Acknowledgements

We are grateful to Yusuke Hirota for his insightful discussions, guidance on the experiments, and careful review of the manuscript.

## References

- Sina Alemohammad, Josue Casco-Rodriguez, Lorenzo Luzi, Ahmed Imtiaz Humayun, Hossein Babaei, Daniel LeJeune, Ali Siahkoobi, and Richard G Baraniuk. Self-consuming generative models go mad. *arXiv preprint arXiv:2307.01850*, 4:14, 2023.
- Anthropic. Claude 3.7 sonnet and claude code. <https://www.anthropic.com/news/claude-3-7-sonnet>, February 2025. Accessed: 2025-05-04.
- Hritik Bansal, Da Yin, Masoud Monajatipoor, and Kai-Wei Chang. How well can text-to-image generative models understand ethical natural language interventions? *arXiv preprint arXiv:2210.15230*, 2022.
- Trupti Bavalatti, Osama Ahmed, Dhaval Potdar, Rakeen Rouf, Faraz Jawed, Manish Kumar Govind, and Siddharth Krishnan. A systematic review of open datasets used in text-to-image (t2i) gen ai model safety. *IEEE Access*, 2025.
- Federico Bianchi, Pratyusha Kalluri, Esin Durmus, Faisal Ladhak, Myra Cheng, Debora Nozza, Tatsunori Hashimoto, Dan Jurafsky, James Zou, and Aylin Caliskan. Easily accessible text-to-image generation amplifies demographic stereotypes at large scale. In *Proceedings of the 2023 ACM Conference on Fairness, Accountability, and Transparency*, pages 1493–1504, 2023.
- Black Forest Labs. Announcing Black Forest Labs. <https://bfl.ai/announcements/24-08-01-bf1>, August 2024. News article; accessed 2025-05-15.
- Manuel Brack, Felix Friedrich, Dominik Hintersdorf, Lukas Struppek, Patrick Schramowski, and Kristian Kersting. Sega: Instructing diffusion using semantic dimensions. *arXiv preprint arXiv:2301.12247*, 2(6), 2023.
- Jun Song Chen, Jincheng Yu, Chongjian Ge, Lewei Yao, Enze Xie, Yue Wu, Zhongdao Wang, James T. Kwok, Ping Luo, Huchuan Lu, and Zhenguo Li. Pixart-alpha: Fast training of diffusion transformer for photorealistic text-to-image synthesis. *International Conference on Learning Representations*, 2023. doi: 10.48550/arxiv.2310.00426.
- Junsong Chen, Yue Wu, Simian Luo, Enze Xie, Sayak Paul, Ping Luo, Hang Zhao, and Zhenguo Li. Pixart-delta: Fast and controllable image generation with latent consistency models, 2024a. URL <https://arxiv.org/abs/2401.05252>.
- Junsong Chen, Chongjian Ge, Enze Xie, Yue Wu, Lewei Yao, Xiaozhe Ren, Zhongdao Wang, Ping Luo, Huchuan Lu, and Zhenguo Li. Pixart-sigma: Weak-to-strong training of diffusion transformer for 4k text-to-image generation. In *European Conference on Computer Vision*, pages 74–91. Springer, 2025a.
- Liang Chen, Shuai Bai, Wenhao Chai, Weichu Xie, Haozhe Zhao, Leon Vinci, Junyang Lin, and Baobao Chang. Multimodal representation alignment for image generation: Text-image interleaved control is easier than you think. *arXiv preprint arXiv:2502.20172*, 2025b.
- Tianwei Chen, Yusuke Hirota, Mayu Otani, Noa García, and Yuta Nakashima. Would deep generative models amplify bias in future models? *Computer Vision and Pattern Recognition*, 2024b. doi: 10.1109/cvpr52733.2024.01030.
- Aditya Chinchure, Pushkar Shukla, Gaurav Bhatt, Kiri Salij, K. Hosanagar, Leonid Sigal, and Matthew Turk. Tibet: Identifying and evaluating biases in text-to-image generative models. *European Conference on Computer Vision*, 2023. doi: 10.48550/arxiv.2312.01261.
- Jaemin Cho, Abhaysinh Zala, and Mohit Bansal. Dall-eval: Probing the reasoning skills and social biases of text-to-image generation models. *IEEE International Conference on Computer Vision*, 2022. doi: 10.1109/iccv51070.2023.00283.
- Kristy Choi, Aditya Grover, Trisha Singh, Rui Shu, and Stefano Ermon. Fair generative modeling via weak supervision. In *International Conference on Machine Learning*, pages 1887–1898. PMLR, 2020.

- Ching-Yao Chuang, Varun Jampani, Yuanzhen Li, Antonio Torralba, and Stefanie Jegelka. Debiasing vision-language models via biased prompts. *arXiv preprint arXiv:2302.00070*, 2023.
- Moreno D’Inca, E. Peruzzo, Massimiliano Mancini, Dejia Xu, Vidit Goel, Xingqian Xu, Zhangyang Wang, Humphrey Shi, and N. Sebe. Openbias: Open-set bias detection in text-to-image generative models. *Computer Vision and Pattern Recognition*, 2024. doi: 10.1109/cvpr52733.2024.01162.
- Alexey Dosovitskiy, Alexey Dosovitskiy, Lucas Beyer, Lucas Beyer, Alexander Kolesnikov, Alexander Kolesnikov, Dirk Weissenborn, Dirk Weissenborn, Xiaohua Zhai, Xiaohua Zhai, Thomas Unterthiner, Thomas Unterthiner, Mostafa Dehghani, Mostafa Dehghani, Matthias Minderer, Matthias Minderer, Georg Heigold, Georg Heigold, Sylvain Gelly, Sylvain Gelly, Jakob Uszkoreit, Jakob Uszkoreit, Neil Houlsby, and Neil Houlsby. An image is worth 16x16 words: Transformers for image recognition at scale. *arXiv: Computer Vision and Pattern Recognition*, 2020. doi: null.
- Patrick Esser, Sumith Kulal, A. Blattmann, Rahim Entezari, Jonas Muller, Harry Saini, Yam Levi, Dominik Lorenz, Axel Sauer, Frederic Boesel, Dustin Podell, Tim Dockhorn, Zion English, Kyle Lacey, Alex Goodwin, Yannik Marek, and Robin Rombach. Scaling rectified flow transformers for high-resolution image synthesis. *International Conference on Machine Learning*, 2024. doi: 10.48550/arxiv.2403.03206.
- Felix Friedrich, Manuel Brack, Lukas Struppek, Dominik Hintersdorf, Patrick Schramowski, Sasha Luccioni, and Kristian Kersting. Fair diffusion: Instructing text-to-image generation models on fairness. *arXiv preprint arXiv:2302.10893*, 2023.
- Sourojit Ghosh and Aylin Caliskan. ‘person’ == light-skinned, western man, and sexualization of women of color: Stereotypes in stable diffusion. *Conference on Empirical Methods in Natural Language Processing*, 2023. doi: 10.18653/v1/2023.findings-emnlp.465.
- Jack Hessel, Ari Holtzman, Maxwell Forbes, Ronan Le Bras, and Yejin Choi. Clipscore: A reference-free evaluation metric for image captioning. *arXiv preprint arXiv:2104.08718*, 2021.
- Martin Heusel, Hubert Ramsauer, Thomas Unterthiner, Bernhard Nessler, and Sepp Hochreiter. Gans trained by a two time-scale update rule converge to a local nash equilibrium. *Advances in neural information processing systems*, 30, 2017.
- Yusuke Hirota, Min-Hung Chen, Chien-Yi Wang, Yuta Nakashima, Yu-Chiang Frank Wang, and Ryo Hachiuma. Saner: Annotation-free societal attribute neutralizer for debiasing clip. *arXiv preprint arXiv:2408.10202*, 2024.
- Jonathan Ho and Tim Salimans. Classifier-free diffusion guidance. *arXiv preprint arXiv:2207.12598*, 2022.
- Jonathan Ho, Ajay Jain, and Pieter Abbeel. Denoising diffusion probabilistic models. In H. Larochelle, M. Ranzato, R. Hadsell, M.F. Balcan, and H. Lin, editors, *Advances in Neural Information Processing Systems*, volume 33, pages 6840–6851. Curran Associates, Inc., 2020. URL [https://proceedings.neurips.cc/paper\\_files/paper/2020/file/4c5bcfec8584af0d967f1ab10179ca4b-Paper.pdf](https://proceedings.neurips.cc/paper_files/paper/2020/file/4c5bcfec8584af0d967f1ab10179ca4b-Paper.pdf).
- Imagen-Team-Google, :, Jason Baldridge, Jakob Bauer, Mukul Bhutani, Nicole Brichtova, Andrew Bunner, Lluís Castrejon, Kelvin Chan, Yichang Chen, Sander Dieleman, Yuqing Du, Zach Eaton-Rosen, Hongliang Fei, Nando de Freitas, Yilin Gao, Evgeny Gladchenko, Sergio Gómez Colmenarejo, Mandy Guo, Alex Haig, Will Hawkins, Hexiang Hu, Huilian Huang, Tobenna Peter Igwe, Christos Kaplanis, Siavash Khodadadeh, Yelin Kim, Ksenia Konyushkova, Karol Langner, Eric Lau, Rory Lawton, Shixin Luo, Soňa Mokrá, Henna Nandwani, Yasumasa Onoe, Aäron van den Oord, Zarana Parekh, Jordi Pont-Tuset, Hang Qi, Rui Qian, Deepak Ramachandran, Poorva Rane, Abdullah Rashwan, Ali Razavi, Robert Riachi, Hansa Srinivasan, Srivatsan Srinivasan, Robin Strudel, Benigno Uria, Oliver Wang, Su Wang, Austin Waters, Chris Wolff, Auriel Wright, Zhisheng Xiao, Hao Xiong, Keyang Xu, Marc van Zee, Junlin Zhang, Katie Zhang, Wenlei Zhou, Konrad Zolna, Ola Aboubakar, Canfer Akbulut, Oscar Akerlund, Isabela Albuquerque, Nina Anderson, Marco Andreetto, Lora Aroyo, Ben Bariach, David Barker, Sherry Ben, Dana Berman, Courtney Biles, Irina Blok, Pankil Botadra, Jenny Brennan, Karla Brown, John Buckley, Rudy Bunel, Elie Bursztein, Christina Butterfield, Ben Caine, Viral Carpenter, Norman Casagrande,



- Ming-Wei Chang, Solomon Chang, Shamik Chaudhuri, Tony Chen, John Choi, Dmitry Churbanau, Nathan Clement, Matan Cohen, Forrester Cole, Mikhail Dektiarev, Vincent Du, Praneet Dutta, Tom Eccles, Ndidi Elue, Ashley Feden, Shlomi Fruchter, Frankie Garcia, Roopal Garg, Weina Ge, Ahmed Ghazy, Bryant Gipson, Andrew Goodman, Dawid Górny, Sven Goyal, Khyatti Gupta, Yoni Halpern, Yena Han, Susan Hao, Jamie Hayes, Jonathan Heek, Amir Hertz, Ed Hirst, Emiel Hoogeboom, Tingbo Hou, Heidi Howard, Mohamed Ibrahim, Dirichi Ike-Njoku, Joana Iljazi, Vlad Ionescu, William Isaac, Reena Jana, Gemma Jennings, Donovan Jenson, Xuhui Jia, Kerry Jones, Xiaoen Ju, Ivana Kajic, Christos Kaplanis, Burcu Karagol Ayan, Jacob Kelly, Suraj Kothawade, Christina Kouridi, Ira Ktena, Jolanda Kumakaw, Dana Kurniawan, Dmitry Lagun, Lily Lavitas, Jason Lee, Tao Li, Marco Liang, Maggie Li-Calis, Yuchi Liu, Javier Lopez Alberca, Matthieu Kim Lorrain, Peggy Lu, Kristian Lum, Yukun Ma, Chase Malik, John Mellor, Thomas Mensink, Inbar Mosseri, Tom Murray, Aida Nematzadeh, Paul Nicholas, Signe Nørly, João Gabriel Oliveira, Guillermo Ortiz-Jimenez, Michela Paganini, Tom Le Paine, Roni Paiss, Alicia Parrish, Anne Peckham, Vikas Peswani, Igor Petrovski, Tobias Pfaff, Alex Pirozhenko, Ryan Poplin, Utsav Prabhu, Yuan Qi, Matthew Rahtz, Cyrus Rashtchian, Charvi Rastogi, Amit Raul, Ali Razavi, Sylvestre-Alvise Rebuffi, Susanna Ricco, Felix Riedel, Dirk Robinson, Pankaj Rohatgi, Bill Rosgen, Sarah Rumbley, Moonkyung Ryu, Anthony Salgado, Tim Salimans, Sahil Singla, Florian Schroff, Candice Schumann, Tanmay Shah, Eleni Shaw, Gregory Shaw, Brendan Shillingford, Kaushik Shivakumar, Dennis Shtatnov, Zach Singer, Evgeny Sluzhaev, Valerii Sokolov, Thibault Sottiaux, Florian Stimberg, Brad Stone, David Stutz, Yu-Chuan Su, Eric Tabellion, Shuai Tang, David Tao, Kurt Thomas, Gregory Thornton, Andeep Toor, Cristian Udrescu, Aayush Upadhyay, Cristina Vasconcelos, Alex Vasiloff, Andrey Voynov, Amanda Walker, Luyu Wang, Miaosen Wang, Simon Wang, Stanley Wang, Qifei Wang, Yuxiao Wang, Ágoston Weisz, Olivia Wiles, Chenxia Wu, Xingyu Federico Xu, Andrew Xue, Jianbo Yang, Luo Yu, Mete Yurtoglu, Ali Zand, Han Zhang, Jiageng Zhang, Catherine Zhao, Adilet Zhaxybay, Miao Zhou, Shengqi Zhu, Zhenkai Zhu, Dawn Bloxwich, Mahyar Bordbar, Luis C. Cobo, Eli Collins, Shengyang Dai, Tulsee Doshi, Anca Dragan, Douglas Eck, Demis Hassabis, Sissie Hsiao, Tom Hume, Koray Kavukcuoglu, Helen King, Jack Krawczyk, Yeqing Li, Kathy Meier-Hellstern, Andras Orban, Yury Pinsky, Amar Subramanya, Oriol Vinyals, Ting Yu, and Yori Zwols. Imagen 3, 2024. URL <https://arxiv.org/abs/2408.07009>.
- Kimmo Karkkainen and Jungseock Joo. Fairface: Face attribute dataset for balanced race, gender, and age for bias measurement and mitigation. In *Proceedings of the IEEE/CVF winter conference on applications of computer vision*, pages 1548–1558, 2021.
- Yeongmin Kim, Byeonghu Na, Minsang Park, Joonho Jang, Dongjun Kim, Wanmo Kang, and Il-Chul Moon. Training unbiased diffusion models from biased dataset. *International Conference on Learning Representations*, 2024. doi: 10.48550/arxiv.2403.01189.
- Davis E King. Max-margin object detection. *arXiv preprint arXiv:1502.00046*, 2015.
- Diederik P. Kingma, Diederik P. Kingma, Max Welling, and Max Welling. Auto-encoding variational bayes. *International Conference on Learning Representations*, 2014. doi: null.
- Junnan Li, Dongxu Li, Silvio Savarese, and Steven Hoi. Blip-2: Bootstrapping language-image pre-training with frozen image encoders and large language models. In *International conference on machine learning*, pages 19730–19742. PMLR, 2023.
- Tsung-Yi Lin, Michael Maire, Serge Belongie, James Hays, Pietro Perona, Deva Ramanan, Piotr Dollár, and C Lawrence Zitnick. Microsoft coco: Common objects in context. In *Computer vision—ECCV 2014: 13th European conference, zurich, Switzerland, September 6–12, 2014, proceedings, part v 13*, pages 740–755. Springer, 2014.
- Y. Lipman, Ricky T. Q. Chen, Heli Ben-Hamu, Maximilian Nickel, and Matt Le. Flow matching for generative modeling. *International Conference on Learning Representations*, 2022. doi: null.
- Yaron Lipman, Marton Havasi, Peter Holderrieth, Neta Shaul, Matt Le, Brian Karrer, Ricky T. Q. Chen, David Lopez-Paz, Heli Ben-Hamu, and Itai Gat. Flow matching guide and code, 2024. URL <https://arxiv.org/abs/2412.06264>.
- Xingchao Liu, Xingchao Liu, Chengyue Gong, Chengyue Gong, Qiang Liu, and Qiang Liu. Flow straight and fast: Learning to generate and transfer data with rectified flow. *International Conference on Learning Representations*, 2022. doi: 10.48550/arxiv.2209.03003.



- Xingchao Liu, Xiwen Zhang, Jianzhu Ma, Jian Peng, et al. Instaflow: One step is enough for high-quality diffusion-based text-to-image generation. In *The Twelfth International Conference on Learning Representations*, 2023.
- Sasha Luccioni, Christopher Akiki, Margaret Mitchell, and Yacine Jernite. Stable bias: Evaluating societal representations in diffusion models. *Neural Information Processing Systems*, 2023. doi: null.
- Abhishek Mandal, Susan Leavy, and Suzanne Little. Generated bias: Auditing internal bias dynamics of text-to-image generative models. *arXiv preprint arXiv:2410.07884*, 2024.
- Ranjita Naik and Besmira Nushi. Social biases through the text-to-image generation lens. In *Proceedings of the 2023 AAAI/ACM Conference on AI, Ethics, and Society*, pages 786–808, 2023.
- OpenAI, Josh Achiam, Steven Adler, Sandhini Agarwal, Lama Ahmad, Ilge Akkaya, Florencia Leoni Aleman, Diogo Almeida, Janko Altenschmidt, Sam Altman, Shyamal Anadkat, Red Avila, Igor Babuschkin, Suchir Balaji, Valerie Balcom, Paul Baltescu, Haiming Bao, Mohammad Bavarian, Jeff Belgum, Irwan Bello, Jake Berdine, Gabriel Bernadett-Shapiro, Christopher Berner, Lenny Bogdonoff, Oleg Boiko, Madelaine Boyd, Anna-Luisa Brakman, Greg Brockman, Tim Brooks, Miles Brundage, Kevin Button, Trevor Cai, Rosie Campbell, Andrew Cann, Brittany Carey, Chelsea Carlson, Rory Carmichael, Brooke Chan, Che Chang, Fotis Chantzis, Derek Chen, Sully Chen, Ruby Chen, Jason Chen, Mark Chen, Ben Chess, Chester Cho, Casey Chu, Hyung Won Chung, Dave Cummings, Jeremiah Currier, Yunxing Dai, Cory Decareaux, Thomas Degry, Noah Deutsch, Damien Deville, Arka Dhar, David Dohan, Steve Dowling, Sheila Dunning, Adrien Ecoffet, Atty Eleti, Tyna Eloundou, David Farhi, Liam Fedus, Niko Felix, Simón Posada Fishman, Juston Forte, Isabella Fulford, Leo Gao, Elie Georges, Christian Gibson, Vik Goel, Tarun Gogineni, Gabriel Goh, Rapha Gontijo-Lopes, Jonathan Gordon, Morgan Grafstein, Scott Gray, Ryan Greene, Joshua Gross, Shixiang Shane Gu, Yufei Guo, Chris Hallacy, Jesse Han, Jeff Harris, Yuchen He, Mike Heaton, Johannes Heidecke, Chris Hesse, Alan Hickey, Wade Hickey, Peter Hoeschele, Brandon Houghton, Kenny Hsu, Shengli Hu, Xin Hu, Joost Huizinga, Shantanu Jain, Shawn Jain, Joanne Jang, Angela Jiang, Roger Jiang, Haozhun Jin, Denny Jin, Shino Jomoto, Billie Jonn, Heewoo Jun, Tomer Kaftan, Łukasz Kaiser, Ali Kamali, Ingmar Kanitscheider, Nitish Shirish Keskar, Tabarak Khan, Logan Kilpatrick, Jong Wook Kim, Christina Kim, Yongjik Kim, Jan Hendrik Kirchner, Jamie Kiros, Matt Knight, Daniel Kokotajlo, Łukasz Kondraciuk, Andrew Kondrich, Aris Konstantinidis, Kyle Kosic, Gretchen Krueger, Vishal Kuo, Michael Lampe, Ikai Lan, Teddy Lee, Jan Leike, Jade Leung, Daniel Levy, Chak Ming Li, Rachel Lim, Molly Lin, Stephanie Lin, Mateusz Litwin, Theresa Lopez, Ryan Lowe, Patricia Lue, Anna Makanju, Kim Malfacini, Sam Manning, Todor Markov, Yaniv Markovski, Bianca Martin, Katie Mayer, Andrew Mayne, Bob McGrew, Scott Mayer McKinney, Christine McLeavey, Paul McMillan, Jake McNeil, David Medina, Aalok Mehta, Jacob Menick, Luke Metz, Andrey Mishchenko, Pamela Mishkin, Vinnie Monaco, Evan Morikawa, Daniel Mossing, Tong Mu, Mira Murati, Oleg Murk, David Mély, Ashvin Nair, Reiichiro Nakano, Rajeev Nayak, Arvind Neelakantan, Richard Ngo, Hyeonwoo Noh, Long Ouyang, Cullen O’Keefe, Jakub Pachocki, Alex Paino, Joe Palermo, Ashley Pantuliano, Giambattista Parascandolo, Joel Parish, Emy Parparita, Alex Passos, Mikhail Pavlov, Andrew Peng, Adam Perelman, Filipe de Avila Belbute Peres, Michael Petrov, Henrique Ponde de Oliveira Pinto, Michael, Pokorný, Michelle Pokrass, Vitchyr H. Pong, Tolly Powell, Alethea Power, Boris Power, Elizabeth Proehl, Raul Puri, Alec Radford, Jack Rae, Aditya Ramesh, Cameron Raymond, Francis Real, Kendra Rimbach, Carl Ross, Bob Rotsted, Henri Roussez, Nick Ryder, Mario Saltarelli, Ted Sanders, Shibani Santurkar, Girish Sastry, Heather Schmidt, David Schnurr, John Schulman, Daniel Selsam, Kyla Sheppard, Toki Sherbakov, Jessica Shieh, Sarah Shoker, Pranav Shyam, Szymon Sidor, Eric Sigler, Maddie Simens, Jordan Sitkin, Katarina Slama, Ian Sohl, Benjamin Sokolowsky, Yang Song, Natalie Staudacher, Felipe Petroski Such, Natalie Summers, Ilya Sutskever, Jie Tang, Nikolas Tezak, Madeleine B. Thompson, Phil Tillet, Amin Tootoonchian, Elizabeth Tseng, Preston Tuggle, Nick Turley, Jerry Tworek, Juan Felipe Cerón Uribe, Andrea Vallone, Arun Vijayvergiya, Chelsea Voss, Carroll Wainwright, Justin Jay Wang, Alvin Wang, Ben Wang, Jonathan Ward, Jason Wei, CJ Weinmann, Akila Welihinda, Peter Welinder, Jiayi Weng, Lilian Weng, Matt Wiethoff, Dave Willner, Clemens Winter, Samuel Wolrich, Hannah Wong, Lauren Workman, Sherwin Wu, Jeff Wu, Michael Wu, Kai Xiao, Tao Xu, Sarah Yoo, Kevin Yu, Qiming Yuan, Wojciech Zaremba, Rowan Zellers, Chong Zhang, Marvin Zhang, Shengjia Zhao, Tianhao Zheng, Juntang Zhuang, William Zhuk, and Barret Zoph. Gpt-4 technical report, 2024. URL <https://arxiv.org/abs/2303.08774>.

- William Peebles and Saining Xie. Scalable diffusion models with transformers. In *Proceedings of the IEEE/CVF International Conference on Computer Vision*, pages 4195–4205, 2023.
- Dustin Podell, Zion English, Kyle Lacey, Andreas Blattmann, Tim Dockhorn, Jonas Müller, Joe Penna, and Robin Rombach. Sdxl: Improving latent diffusion models for high-resolution image synthesis, 2023.
- Alec Radford, Jong Wook Kim, Chris Hallacy, Aditya Ramesh, Gabriel Goh, Sandhini Agarwal, Girish Sastry, Amanda Askell, Pamela Mishkin, Jack Clark, et al. Learning transferable visual models from natural language supervision. In *International conference on machine learning*, pages 8748–8763. PMLR, 2021.
- Colin Raffel, Noam Shazeer, Adam Roberts, Katherine Lee, Sharan Narang, Michael Matena, Yanqi Zhou, Wei Li, and Peter J Liu. Exploring the limits of transfer learning with a unified text-to-text transformer. *Journal of machine learning research*, 21(140):1–67, 2020.
- R. Rombach, A. Blattmann, D. Lorenz, P. Esser, and B. Ommer. High-resolution image synthesis with latent diffusion models. In *2022 IEEE/CVF Conference on Computer Vision and Pattern Recognition (CVPR)*, pages 10674–10685, Los Alamitos, CA, USA, jun 2022a. IEEE Computer Society. doi: 10.1109/CVPR52688.2022.01042. URL <https://doi.ieeecomputersociety.org/10.1109/CVPR52688.2022.01042>.
- Robin Rombach, Andreas Blattmann, Dominik Lorenz, Patrick Esser, and Björn Ommer. High-resolution image synthesis with latent diffusion models. In *Proceedings of the IEEE/CVF conference on computer vision and pattern recognition*, pages 10684–10695, 2022b.
- Olaf Ronneberger, Philipp Fischer, and Thomas Brox. U-net: Convolutional networks for biomedical image segmentation. In *Medical image computing and computer-assisted intervention–MICCAI 2015: 18th international conference, Munich, Germany, October 5-9, 2015, proceedings, part III 18*, pages 234–241. Springer, 2015.
- Teresa Sandoval-Martin and Ester Martínez-Sanzo. Perpetuation of gender bias in visual representation of professions in the generative ai tools dall·e and bing image creator. *Social Sciences*, 13(5): 250, 2024.
- Axel Sauer, Dominik Lorenz, A. Blattmann, and Robin Rombach. Adversarial diffusion distillation. *European Conference on Computer Vision*, 2023. doi: 10.48550/arxiv.2311.17042.
- Axel Sauer, Frederic Boesel, Tim Dockhorn, Andreas Blattmann, Patrick Esser, and Robin Rombach. Fast high-resolution image synthesis with latent adversarial diffusion distillation. In *SIGGRAPH Asia 2024 Conference Papers*, pages 1–11, 2024.
- Christoph Schuhmann, Romain Beaumont, Richard Vencu, Cade Gordon, Ross Wightman, Mehdi Cherti, Theo Coombes, Aarush Katta, Clayton Mullis, Mitchell Wortsman, et al. Laion-5b: An open large-scale dataset for training next generation image-text models. *Advances in Neural Information Processing Systems*, 35:25278–25294, 2022.
- Ashish Seth, Mayur Hemani, and Chirag Agarwal. Dear: Debiasing vision-language models with additive residuals. In *Proceedings of the IEEE/CVF Conference on Computer Vision and Pattern Recognition (CVPR)*, pages 6820–6829, June 2023.
- Jascha Sohl-Dickstein, Eric Weiss, Niru Maheswaranathan, and Surya Ganguli. Deep unsupervised learning using nonequilibrium thermodynamics. In *International conference on machine learning*, pages 2256–2265. PMLR, 2015.
- Yang Song, Yang Song, Yang Song, Yang Song, Jascha Sohl-Dickstein, Jascha Sohl-Dickstein, Diederik P. Kingma, Diederik P. Kingma, Abhishek Kumar, Abhishek Kumar, Abhishek Kumar, Abhishek Kumar, Stefano Ermon, Stefano Ermon, Ben Poole, and Ben Poole. Score-based generative modeling through stochastic differential equations. *arXiv: Learning*, 2020. doi: null.
- Yingtian Tang, Yutaro Yamada, Yoyo Zhang, and Ilker Yildirim. When are lemons purple? the concept association bias of vision-language models. In *Proceedings of the 2023 Conference on Empirical Methods in Natural Language Processing*, pages 14333–14348, 2023.

- Ashish Vaswani, Noam Shazeer, Niki Parmar, Jakob Uszkoreit, Llion Jones, Aidan N Gomez, Łukasz Kaiser, and Illia Polosukhin. Attention is all you need. In I. Guyon, U. Von Luxburg, S. Bengio, H. Wallach, R. Fergus, S. Vishwanathan, and R. Garnett, editors, *Advances in Neural Information Processing Systems*, volume 30. Curran Associates, Inc., 2017. URL [https://proceedings.neurips.cc/paper\\_files/paper/2017/file/3f5ee243547dee91fbd053c1c4a845aa-Paper.pdf](https://proceedings.neurips.cc/paper_files/paper/2017/file/3f5ee243547dee91fbd053c1c4a845aa-Paper.pdf).
- Yixin Wan, Arjun Subramonian, Anaelia Ovalle, Zongyu Lin, Ashima Suvana, Christina Chance, Hritik Bansal, Rebecca Pattichis, and Kai-Wei Chang. Survey of bias in text-to-image generation: Definition, evaluation, and mitigation. *arXiv preprint arXiv:2404.01030*, 2024.
- Jialu Wang, X Liu, Zonglin Di, Yang Liu, and Xin Eric Wang. T2iat: Measuring valence and stereotypical biases in text-to-image generation. *Annual Meeting of the Association for Computational Linguistics*, 2023. doi: 10.48550/arxiv.2306.00905.
- Yankun Wu, Yuta Nakashima, and Noa García. Stable diffusion exposed: Gender bias from prompt to image. *Proceedings of the AAAI/ACM Conference on AI, Ethics, and Society*, 2023. doi: 10.48550/arxiv.2312.03027.
- Sierra Wyllie, Ilia Shumailov, and Nicolas Papernot. Fairness feedback loops: training on synthetic data amplifies bias. In *Proceedings of the 2024 ACM Conference on Fairness, Accountability, and Transparency*, pages 2113–2147, 2024.
- Song Yang, Prafulla Dhariwal, Mark Chen, and Ilya Sutskever. Consistency models. *International Conference on Machine Learning*, 2023. doi: 10.48550/arxiv.2303.01469.
- Jiahui Yu, Yuanzhong Xu, Jing Yu Koh, Thang Luong, Gunjan Baid, Zirui Wang, Vijay Vasudevan, Alexander Ku, Yinfei Yang, Burcu Karagol Ayan, et al. Scaling autoregressive models for content-rich text-to-image generation. *arXiv preprint arXiv:2206.10789*, 2(3):5, 2022.
- Beichen Zhang, Pan Zhang, Xiaoyi Dong, Yuhang Zang, and Jiaqi Wang. Long-clip: Unlocking the long-text capability of clip. In *European Conference on Computer Vision*, pages 310–325. Springer, 2024.
- Cheng Zhang, Xuanbai Chen, Siqi Chai, Chen Henry Wu, Dmitry Lagun, Thabo Beeler, and Fernando De la Torre. Iti-gen: Inclusive text-to-image generation. In *Proceedings of the IEEE/CVF International Conference on Computer Vision*, pages 3969–3980, 2023.

## Technical Appendices and Supplementary Material

### A Proof of Proposition 1

**Proposition 1.** *Let  $\mathbf{y}$  represent the input text,  $\mathbf{x}$  the generated image, and  $\mathbf{z}$  the latent attribute, and assume conditional independence between  $\mathbf{x}$  and  $\mathbf{z}$  given  $\mathbf{y}$ , the following equation holds:*

$$\nabla_{\mathbf{x}} \log p(\mathbf{x} | \mathbf{y}) = \sum_{z \in Z} p(\mathbf{z} = z | \mathbf{y}) \nabla_{\mathbf{x}} \log p(\mathbf{x} | \mathbf{z} = z, \mathbf{y}).$$

*Proof.* We start from the left-hand side (LHS) of the equation stated in Proposition 1.

$$\begin{aligned} \nabla_{\mathbf{x}} \log p(\mathbf{x} | \mathbf{y}) &= \frac{1}{p(\mathbf{x} | \mathbf{y})} \nabla_{\mathbf{x}} p(\mathbf{x} | \mathbf{y}) && \text{(Using the chain rule for logarithms)} \\ &= \frac{1}{p(\mathbf{x} | \mathbf{y})} \nabla_{\mathbf{x}} \sum_{z \in Z} p(\mathbf{x}, \mathbf{z} = z | \mathbf{y}) && \text{(Marginalizing over } \mathbf{z}) \\ &= \frac{1}{p(\mathbf{x} | \mathbf{y})} \nabla_{\mathbf{x}} \sum_{z \in Z} p(\mathbf{x} | \mathbf{z} = z, \mathbf{y}) p(\mathbf{z} = z | \mathbf{y}) && \text{(Using the definition of conditional probability)} \\ &= \frac{1}{p(\mathbf{x} | \mathbf{y})} \sum_{z \in Z} p(\mathbf{z} = z | \mathbf{y}) \nabla_{\mathbf{x}} p(\mathbf{x} | \mathbf{z} = z, \mathbf{y}) && \text{(Linearity of } \nabla_{\mathbf{x}}) \\ &= \sum_{z \in Z} \frac{p(\mathbf{z} = z | \mathbf{y})}{p(\mathbf{x} | \mathbf{y})} \nabla_{\mathbf{x}} p(\mathbf{x} | \mathbf{z} = z, \mathbf{y}). \end{aligned}$$

Then we apply Bayes' theorem,

$$p(\mathbf{z} = z | \mathbf{x}, \mathbf{y}) = \frac{p(\mathbf{z} = z | \mathbf{y}) p(\mathbf{x} | \mathbf{z} = z, \mathbf{y})}{p(\mathbf{x} | \mathbf{y})},$$

to obtain

$$\begin{aligned} \nabla_{\mathbf{x}} \log p(\mathbf{x} | \mathbf{y}) &= \sum_{z \in Z} \frac{p(\mathbf{z} = z | \mathbf{x}, \mathbf{y})}{p(\mathbf{x} | \mathbf{z} = z, \mathbf{y})} \nabla_{\mathbf{x}} p(\mathbf{x} | \mathbf{z} = z, \mathbf{y}) \\ &= \sum_{z \in Z} p(\mathbf{z} = z | \mathbf{x}, \mathbf{y}) \nabla_{\mathbf{x}} \log p(\mathbf{x} | \mathbf{z} = z, \mathbf{y}). \end{aligned} \quad \text{(Using the chain rule for logarithms)}$$

Finally, we apply the conditional independence assumption given in the proposition,  $p(\mathbf{z} = z | \mathbf{x}, \mathbf{y}) = p(\mathbf{z} = z | \mathbf{y})$ :

$$\nabla_{\mathbf{x}} \log p(\mathbf{x} | \mathbf{y}) = \sum_{z \in Z} p(\mathbf{z} = z | \mathbf{y}) \nabla_{\mathbf{x}} \log p(\mathbf{x} | \mathbf{z} = z, \mathbf{y}).$$

□

### B Details for Societal Bias Mitigation Experiment

#### B.1 Evaluation dataset details

For efficient evaluation, we used a subset of 50 randomly selected profession names from the full stable bias dataset Luccioni et al. [2023] for each evaluation trial. Table 6 presents a list of the 50 professions used for evaluation.

#### B.2 Evaluation metric details

The FairFace classifier outputs two gender categories, *male* and *female*, and seven race categories, *White*, *Southeast Asian*, *Middle Eastern*, *Latino\_Hispanic*, *Indian*, *East Asian*, and *Black*. Based on these classification results, we compute the statistical parity against the target distributions. Table 7

| Professions                |                         |                    |                     |
|----------------------------|-------------------------|--------------------|---------------------|
| aerospace engineer         | aide                    | author             | bartender           |
| carpenter                  | cashier                 | CEO                | civil engineer      |
| cleaner                    | coach                   | compliance officer | cook                |
| dental assistant           | dentist                 | detective          | electrical engineer |
| engineer                   | facilities manager      | fast food worker   | file clerk          |
| graphic designer           | hairdresser             | head cook          | health technician   |
| industrial engineer        | interior designer       | interviewer        | inventory clerk     |
| jailer                     | machinery mechanic      | manicurist         | massage therapist   |
| medical records specialist | mental health counselor | metal worker       | office clerk        |
| painter                    | payroll clerk           | physical therapist | plane mechanic      |
| postal worker              | psychologist            | purchasing agent   | repair worker       |
| roofer                     | sales manager           | sheet metal worker | social worker       |
| underwriter                | welder                  |                    |                     |

Table 6: A 50 profession subset of the stable bias professions dataset used in the experiment. The subset is randomly selected from the full dataset.

| Occupation          | Female (%) | Male (%) | White (%) | Black (%) | Asian (%) | Hispanic (%) |
|---------------------|------------|----------|-----------|-----------|-----------|--------------|
| CEO                 | 33.0       | 67.0     | 82.2      | 5.8       | 6.1       | 5.8          |
| Doctor              | 44.5       | 55.5     | 64.6      | 7.0       | 22.2      | 6.2          |
| Computer Programmer | 17.8       | 82.2     | 65.7      | 8.3       | 16.0      | 10.1         |
| Nurse               | 86.8       | 13.2     | 67.0      | 14.7      | 9.1       | 9.1          |
| Housekeeper         | 87.7       | 12.3     | 51.3      | 10.2      | 3.1       | 35.3         |

Table 7: Gender and race distributions from BLS 2024 statistics. Race percentages have been normalized so that they sum to 100 %.

shows the 2024 BLS employment statistics <sup>2</sup> for *CEO*, *computer programmer*, *doctor*, *nurse*, and *housekeeper*. The original statistics report the percent of total employed for women, *White*, *Black or African American*, *Asian*, and *Hispanic or Latino*. To construct the BLS target distribution, we assigned the proportion of women to the probability of *female* and one minus that proportion to *male* in the gender category. For the race categories, we normalized the proportions for *White*, *Black or African American*, *Asian*, and *Hispanic or Latino* so that they sum to one <sup>3</sup> and used this as the target distribution. Because the FairFace classifier does not include a generic *Asian* category, we combined the probabilities of *Southeast Asian* and *East Asian* to represent *Asian* when computing statistical parity.

### B.3 ENTIGEN setup details

As an ethical intervention to promote equitable judgment in T2I models, we added “, *if all individuals can be <PROFESSION> irrespective of their gender and race*” to the end of the input prompt.

### B.4 Fair Diffusion setup details

For gender editing, we predefined the prompts [“*male person*”, “*female person*”, “*non-binary person*”], and for race editing, the prompts [“*white person*”, “*black person*”, “*asian person*”, “*latino person*”, “*indian person*”]. During sampling, one gender prompt and one race prompt were drawn according to the target distribution, and `reverse_editing_direction=True` was used to enhance the selected attribute while suppressing the others. All editing operations employed the following hyperparameters (as in the original implementation):

- `edit_warmup_steps = 1`
- `edit_guidance_scale = 3.0`

<sup>2</sup><https://www.bls.gov/cps/cpsaat11.htm>

<sup>3</sup>NOTE: Estimates for the above race groups (*White*, *Black or African American*, and *Asian*) do not sum to totals because data are not presented for all races. Persons whose ethnicity is identified as *Hispanic or Latino* may be of any race.

- `edit_threshold = 0.95`
- `edit_weights = 1.0`
- `edit_momentum_scale = 0.3`
- `edit_momentum_beta = 0.6`

Except for these settings, all other parameters matched those of the original work Friedrich et al. [2023].

## B.5 FairT2I setup details

T2I model sampling was performed using `PNDMScheduler` with 50 sampling steps. The `guidance_scale` for classifier-free guidance was set to 7.5. During inference, we set the batch size to 200 and image resolution  $512 \times 512$ , and a single inference on one NVIDIA H100 GPU took approximately 4 minutes.

For bias detection, we used `claude-3-7-sonnet-20250219`, and for prompt rewriting, we used `gpt-4o-mini-2024-07-18`.

The prompt used for LLM-assisted bias detection is as follows:

- When a prompt is provided, image generation AI often supplements the image with information not explicitly mentioned in the prompt, influenced by biases learned from its training data.

- Analyze the potential biases that may be present in an image generated based on the given prompt.

- For each bias, specify its category (e.g., gender, race, age, time, color, etc.) and list ALL relevant elements (e.g., for "gender", elements could include "male", "female", "non-binary").

- Think carefully so that you do not miss any biases.

- Never add human-related bias categories if the prompt has nothing to do with human.

- Provide the analysis strictly in JSON format. Do not include any text outside of the JSON output. For example:

```

{{
  "gender": ["male", "female", "non-binary"],
  "age": ["child", "teen", "young adult", "middle-aged", "elderly"],
  ...
}}
```

- Exclude any key whose value list contains only a single element.

- Here is the input:  
 Prompt: <PROMPT>

The following prompt was used for the LLM-assisted fusion of the textual input  $y$  and the latent attribute  $z$ :

- Please rewrite the following prompt to naturally include the specified attributes.

- Ensure you only incorporate the original content and the given attributes, without adding any other unnecessary elements or conversational text.

Original prompt: <TEXTUAL INPUT>

Attributes to include: <SAMPLED SENSITIVE ATTRIBUTE>

Rewritten prompt:

## B.6 Statistical significance test methodology

To determine if FairT2I achieved statistically significantly lower SP scores compared to another method (denoted as Method A), we employed a one-sided non-parametric bootstrap hypothesis test with  $N_{boot} = 1000$  iterations. In each iteration  $i$ , demographic classifications were resampled with

replacement from the set of generated images for Method A and FairT2I, maintaining the original sample sizes from which the SP scores were computed. Specifically:

- For the **uniform distribution target** (see Section B.7), overall SP scores were initially calculated from demographic classifications of all 50 occupations  $\times$  200 images/occupation = 10,000 images generated per method. The bootstrap procedure then resampled from these 10,000 image classifications for each method to generate bootstrap SP scores.
- For the **BLS statistics target** (see Section B.8), SP scores were initially calculated for each occupation based on the  $n = 200$  images generated per occupation per method. The bootstrap procedure then resampled from the 200 image classifications for a given occupation for each method.

SP scores were then calculated for these bootstrap samples ( $SP_{A,i}^*$  for Method A and  $SP_{B,i}^*$  for FairT2I, where B denotes FairT2I). The difference  $D_i^* = SP_{A,i}^* - SP_{B,i}^*$  was computed for each iteration. The  $p$ -value was estimated as the proportion of these bootstrap differences  $D_i^*$  that were less than or equal to zero:  $p = \frac{\sum_{i=1}^{N_{boot}} \mathbb{I}(D_i^* \leq 0)}{N_{boot}}$ , where  $\mathbb{I}(\cdot)$  is the indicator function. This  $p$ -value tests the null hypothesis  $H_0 : SP_{FairT2I} \geq SP_{Method A}$  against the alternative hypothesis  $H_A : SP_{FairT2I} < SP_{Method A}$ .  $p < 0.05$  indicates that FairT2I is significantly better than Method A for the given SP metric.

### B.7 Detailed results of uniform distribution target

The overall SP scores for gender and race when targeting a uniform distribution are presented in Table 8. The statistical significance of FairT2I’s scores compared to other methods was assessed using the bootstrap test described in Section B.6.

Table 8: Gender SP (left) and Race SP (right) scores (lower is better) from the uniform distribution. For each metric, the best score is shown in **bold**. For Original, ENTIGEN, and FairDiffusion, the  $p$ -value in parentheses ( $p$ -val) indicates if FairT2I (Ours) is significantly better than that method ( $p < 0.05$  highlighted in **bold** for  $SP_{FairT2I} < SP_{Method}$ ).

| Method         | Gender SP ↓               | Race SP ↓                 |
|----------------|---------------------------|---------------------------|
| Original       | 0.2056 (< <b>0.0001</b> ) | 0.3907 (< <b>0.0001</b> ) |
| ENTIGEN        | 0.0661 (< <b>0.0001</b> ) | 0.2001 (< <b>0.0001</b> ) |
| FairDiffusion  | 0.2083 (< <b>0.0001</b> ) | 0.3137 (< <b>0.0001</b> ) |
| FairT2I (Ours) | <b>0.0123</b>             | <b>0.1864</b>             |

**Discussion of uniform distribution results.** As shown in Table 8, when targeting a uniform demographic distribution across all occupations, FairT2I (Ours) achieved the best overall SP scores for both Gender SP (0.0123) and Race SP (0.1864). The statistical significance tests, detailed in Section B.6, confirm these improvements. FairT2I is shown to be significantly better than the Original method (Gender SP: 0.2056, Race SP: 0.3907), ENTIGEN (Gender SP: 0.0661, Race SP: 0.2001), and FairDiffusion (Gender SP: 0.2083, Race SP: 0.3137) for both metrics, with all associated  $p$ -values being less than 0.000. This indicates a strong and statistically robust improvement in fairness for overall image generation when a uniform distribution is the goal.

### B.8 Detailed results of BLS statistics target

For the BLS statistics target, FairT2I’s performance in achieving lower SP scores per occupation was also evaluated against other methods. The statistical significance of these comparisons was determined using the one-sided non-parametric bootstrap hypothesis test detailed in Section B.6. The SP scores and the corresponding  $p$ -values from these tests are presented in Table 9.

**Discussion of BLS statistics results.** The analyses in Table 9 indicate that FairT2I generally achieves lower SP scores for both gender and race attributes compared to existing methods when targeting BLS statistics. For **Gender SP**, FairT2I consistently demonstrates statistically significant improvements ( $p < 0.05$ ) over the Original method across all five occupations. It also shows significant advantages over FairDiffusion in most occupations (*CEO, computer programmer, nurse, housekeeper*). Compared

Table 9: Gender SP (top) and Race SP (bottom) scores (lower is better) when targeting BLS statistics. For each metric and occupation, the best score is shown in **bold**. For Original, ENTIGEN, and FairDiffusion, the  $p$ -value in parentheses ( $p$ -val) indicates if FairT2I (Ours) is significantly better than that method ( $p < 0.05$  highlighted in **bold** for  $SP_{\text{FairT2I}} < SP_{\text{Method}}$ ).

| Gender SP ↓    |                         |                         |                         |                         |                         |
|----------------|-------------------------|-------------------------|-------------------------|-------------------------|-------------------------|
| Method         | CEO                     | comp. prog.             | doctor                  | nurse                   | housekeeper             |
| Original       | 0.3637 ( <b>0.000</b> ) | 0.1651 ( <b>0.000</b> ) | 0.3843 ( <b>0.000</b> ) | 0.1796 ( <b>0.001</b> ) | 0.1459 ( <b>0.000</b> ) |
| ENTIGEN        | 0.3748 ( <b>0.000</b> ) | 0.0569 (0.254)          | 0.1229 (0.123)          | 0.1210 ( <b>0.044</b> ) | <b>0.0121</b> (0.547)   |
| FairDiffusion  | 0.1956 ( <b>0.022</b> ) | 0.1089 ( <b>0.044</b> ) | 0.1138 (0.206)          | 0.1653 ( <b>0.004</b> ) | 0.1597 ( <b>0.000</b> ) |
| FairT2I (Ours) | <b>0.0710</b>           | <b>0.0170</b>           | <b>0.0550</b>           | <b>0.0537</b>           | <b>0.0121</b>           |

| Race SP ↓      |                         |                         |                         |                         |                         |
|----------------|-------------------------|-------------------------|-------------------------|-------------------------|-------------------------|
| Method         | CEO                     | comp. prog.             | doctor                  | nurse                   | housekeeper             |
| Original       | 0.6050 ( <b>0.000</b> ) | 0.2213 ( <b>0.003</b> ) | 0.2110 ( <b>0.016</b> ) | 0.1971 (0.234)          | 1.0207 ( <b>0.000</b> ) |
| ENTIGEN        | 0.5004 ( <b>0.000</b> ) | 0.6115 ( <b>0.000</b> ) | 0.4727 ( <b>0.000</b> ) | 0.4805 ( <b>0.000</b> ) | 0.9341 ( <b>0.000</b> ) |
| FairDiffusion  | 0.1664 ( <b>0.019</b> ) | 0.1484 ( <b>0.027</b> ) | <b>0.0750</b> (0.752)   | <b>0.1285</b> (0.714)   | 0.3074 ( <b>0.008</b> ) |
| FairT2I (Ours) | <b>0.0677</b>           | <b>0.0886</b>           | 0.1137                  | 0.1540                  | <b>0.2001</b>           |

to ENTIGEN, FairT2I provides significant improvements in two occupations (*CEO*, *nurse*), while for others, including a tied best performance with ENTIGEN for *housekeeper*, the differences were not statistically significant. Regarding **Race SP**, FairT2I shows robust and statistically significant improvements over ENTIGEN across all occupations. Against the Original method, FairT2I is significantly better in four out of five occupations. When compared with FairDiffusion, FairT2I offers significant gains for three occupations (*CEO*, *computer programmer*, *housekeeper*). Notably, FairDiffusion achieved lower Race SP scores for the *doctor* and *nurse* occupations, where FairT2I did not show a significant advantage.

**Stacked bar chart visualization.** Figure 5 presents stacked bar charts comparing demographic distributions of target BLS statistics and empirical distributions across five occupations. Visually, FairT2I generally demonstrates a closer alignment to the target BLS distributions for both gender and race across most occupations.

## C Details for Diversity Control Experiment

### C.1 Evaluation dataset details

For efficient evaluation, we used a subset of 50 randomly selected profession names from the full Parti Prompt dataset Yu et al. [2022] for each evaluation trial. Table 10 presents a list of the 50 professions used for evaluation.

### C.2 Evaluation metrics details

This section provides further details on the implementation of the evaluation metrics used in Section 5 to assess image fidelity, text-image alignment, and diversity. For all trace-based diversity metrics, we generated 200 images for each of the 50 sampled Parti Prompts. Image features were extracted from these 200 images, and the trace of their covariance matrix was computed.

**FID.** We calculated FID Heusel et al. [2017] to assess image fidelity against the COCO Karpathy test split [Lin et al., 2014]. We used the PyTorch implementation of FID from the `pytorch-fid` library<sup>4</sup>.

**CLIPScore.** To evaluate text-image alignment, we computed CLIPScore Hessel et al. [2021].

- **Model and Library:** We utilized the OpenAI CLIP ViT-B/32 model, accessed via the official `clip` Python package.

<sup>4</sup><https://github.com/mseitzer/pytorch-fid>



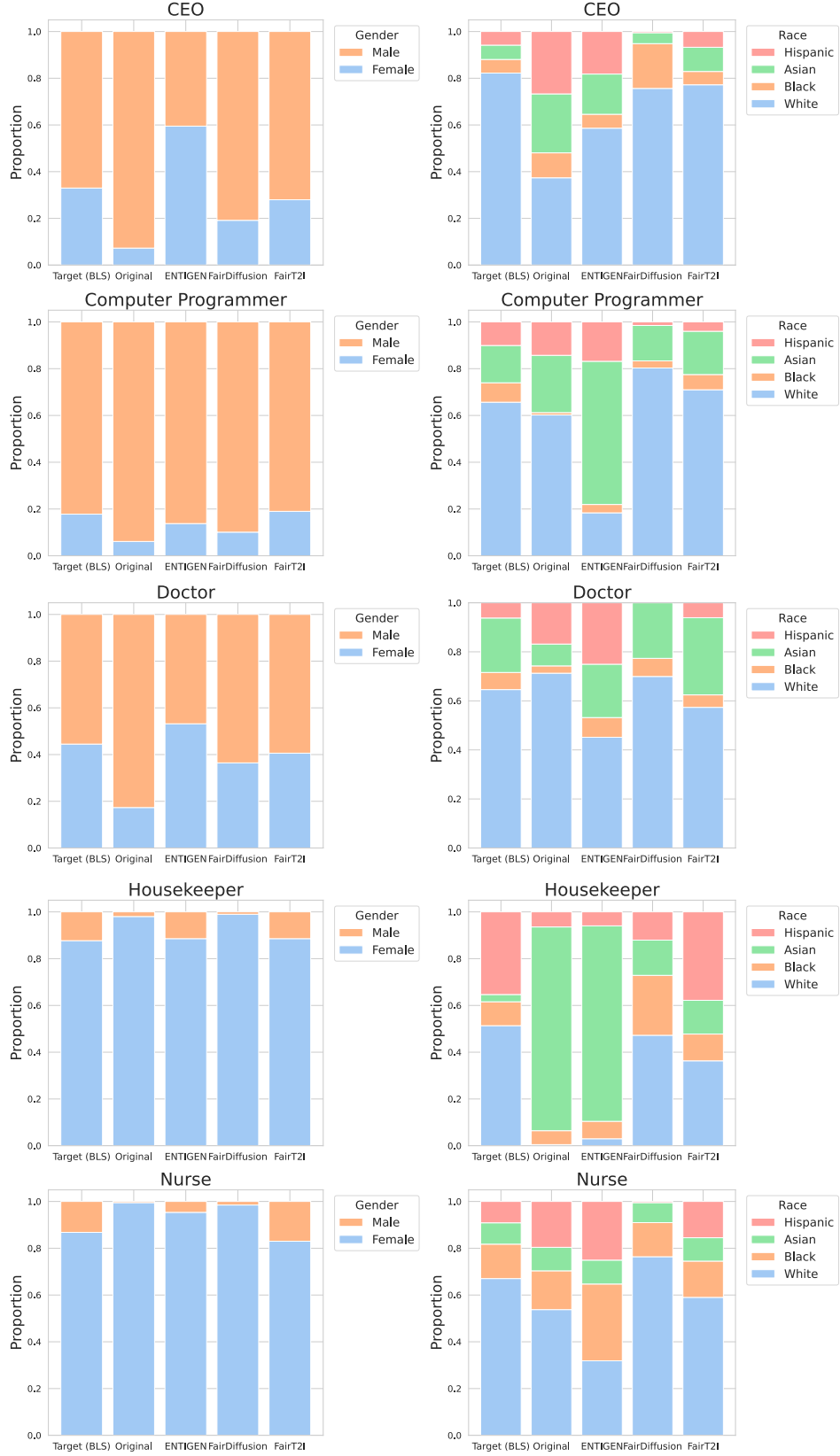


Figure 5: Comparison of the target BLS statistics and empirical distributions produced by original Stable Diffusion, ENTIGEN, FairDiffusion and FairT2I (Ours) for gender (left) and race (right), shown as stacked bar charts.

Table 10: A 50 prompt subset of the Parti Prompt dataset used in the experiment. The subset is randomly selected from the full dataset.

| No. Description   | No. Description  |
|---|--|
| 1. a pile of cash on a wooden table                                       | 26. a paranoid android freaking out and jumping into the air because it is surrounded by colorful Easter eggs                        |
| 2. five frosted glass bottles   | 27. a musical note   |
| 3. a view of the Big Dipper in the night sky                              | 28. Anubis wearing sunglasses and sitting astride a hog motorcyle  |
| 4. a cow  | 29. a photograph of a squirrel holding an arrow above its head and holding a longbow in its left hand                                |
| 5. a Ferrari Testarossa in front of the Kremlin                           | 30. an elder politician giving a campaign speech   |
| 6. a rowboat  | 31. a hot air balloon with a yin-yang symbol   |
| 7. a portrait of a postal worker who has forgotten their mailbag          | 32. overhead view of three people looking down at the street from the top of a tall building   |
| 8. a helicopter hovering over Times Square                                | 33. meaning of life  |
| 9. a t-shirt with Carpe Diem written on it                                | 34. a laptop no letters on its keyboard  |
| 10. a canal in Venice   | 35. a glass of orange juice with an orange peel stuck on the rim   |
| 11. trees seen through a car window on a rainy day                        | 36. a yellow tiger with blue stripes   |
| 12. a grumpy porcupine handing a check for \$10                           | 37. cash   |
| 13. a watermelon chair  | 38. matching socks with cute cats on them  |
| 14. a triangle with a smiling face  | 39. five chairs  |
| 15. Four deer surrounding a moose.  | 40. an airplane flying into a cloud that looks like monster  |
| 16. an old red truck parked by the geyser Old Faithful                    | 41. a long-island ice tea cocktail next to a napkin  |
| 17. a tree surrounded by flowers  | 42. a white robot passing a soccer ball to a red robot   |
| 18. A photo of a Ming Dynasty vase on a leather topped table.             | 43. a black towel  |
| 19. a chair   | 44. a capybara   |
| 20. a wooden post   | 45. artificial intelligence  |
| 21. Jupiter rises on the horizon.   | 46. Portrait of a tiger wearing a train conductor's hat and holding a skateboard that has a yin-yang symbol on it. charcoal sketch   |
| 22. A raccoon wearing formal clothes                                      | 47. Anime illustration of the Great Pyramid sitting next to the Parthenon under a blue night sky of roiling energy                   |
| 23. A bowl of soup that looks like a monster with tofu says deep learning | 48. a chess queen to the right of a chess knight   |
| 24. the Mona Lisa in the style of Minecraft                               | 49. a Tyrannosaurus Rex roaring in front of a palm tree  |
| 25. a sphere  | 50. Portrait of a gecko wearing a train conductor's hat and holding a flag that has a yin-yang symbol on it. Child's crayon drawing. |

- **Feature Extraction:** For each (prompt, generated image) pair, the prompt text was encoded using `model.encode_text()` and the image was encoded using `model.encode_image()`. Both encoders produce L2-normalized features.
- **Score Calculation:** The CLIPScore for a single pair is the dot product of their respective normalized feature embeddings.
- **Aggregation:** The final reported CLIPScore for a given prompt is the average score across all 200 images generated for that prompt.

**CLIP Trace.** To quantify diversity using CLIP Radford et al. [2021] features, we calculated the trace of the covariance matrix of image embeddings.

- **Model and Library:** We used the OpenAI CLIP ViT-B/32 model, via the `clip` Python package.
- **Feature Extraction:** For each of the 50 sampled prompts, we generated 200 images. All 200 images were encoded into L2-normalized feature vectors using `model.encode_image()` with a batch size of 32. This resulted in a set of 200 feature vectors per prompt.
- **Trace Calculation:** For each prompt, we computed the covariance matrix of these 200 feature vectors using `numpy.cov(features, rowvar=False)`. The CLIP Trace diversity metric is the trace of this covariance matrix, calculated using `numpy.trace()`.

**BLIP2 Trace.** Similar to CLIP Trace, we also quantified diversity using BLIP-2 Li et al. [2023] features.

- **Model and Library:** We employed the Salesforce/blip2-opt-2.7b model, accessed via the Hugging Face transformers library, specifically using `Blip2Processor` for preprocessing and `Blip2Model` for feature extraction.
- **Feature Extraction:** For each prompt, the 200 generated images were processed. Image features were obtained from the `pooler_output` of `model.get_image_features()`.
- **Trace Calculation:** Analogous to CLIP Trace, for each prompt, we computed the covariance matrix of the 200 BLIP-2 image feature vectors and then calculated its trace.

### C.3 FairT2I setup details

T2I model sampling was performed using `FlowMatchEulerDiscreteScheduler` with 28 sampling steps. The `guidance_scale` for classifier-free guidance was set to 4.0. During inference, we set the batch size to 200 and image resolution  $1024 \times 1024$ , and a single inference on one NVIDIA H100 GPU took approximately 4 minutes.

For bias detection, we used `claude-3-7-sonnet-20250219`, and for prompt rewriting, we used `gpt-4o-mini-2024-07-18`.

The prompt used for LLM-assisted bias detection is as follows:

- When a prompt is provided, image generation AI often supplements the image with information not explicitly mentioned in the prompt, influenced by biases learned from its training data.
- Your goal is to identify potential characteristics an AI might assume or interpolate for features NOT explicitly stated in the prompt.
- Analyze these potential assumed characteristics (biases) that may be present in an image generated based on the given prompt.
- **CRITICAL RULE:** Do NOT identify a characteristic category as a "bias" if that characteristic is already explicitly defined or specified in the input prompt. For example, if the prompt is "a tall tree", 'height' or 'size' is NOT a bias because "tall" (a descriptor of its heightsize) is specified. Similarly, if a prompt mentioned "a character wearing a blue hat", 'color of the hat' is not a bias. A bias in this context only refers to unspecified attributes that the AI must infer.

- For each identified potential bias (unspecified characteristic), specify its category (e.g., gender, race, age, material, texture, setting, artistic\_style, era, etc.) and list ALL relevant elements (e.g., for "artistic\_style", elements could include "photorealistic", "cartoonish", "impressionistic", "abstract", "watercolor").
- Think carefully so that you do not miss any potential unspecified characteristics that an AI might interpolate.
- Never add human-related bias categories (like gender, race, age) if the prompt has nothing to do with human subjects. For example, a prompt about "a quiet forest" should not include "gender" as a bias category.
- Provide the analysis strictly in JSON format. Do not include any text outside of the JSON output. For example:  

```
{{ "artistic_style": ["photorealistic", "cartoonish", "impressionistic", "abstract", "watercolor"],  
  "time_of_day": ["morning", "noon", "afternoon", "evening", "night"],  
  "weather_conditions": ["sunny", "cloudy", "rainy", "snowy", "foggy"] }}
```
- Exclude any key whose value list contains only a single element.
- Here is the input:  
Prompt: <PROMPT>

We utilized the same prompt for integration of the input text  $y$  and the sensitive attribute  $z$  with B.5.

#### C.4 Statistical significance test methodology

To assess the statistical significance of the differences observed in diversity (BLIP2 Trace, CLIP Trace) and text-image alignment (CLIP Score) metrics (see Section 5 in the main paper), we performed one-sided Mann-Whitney U tests. This non-parametric test was chosen as it does not assume a specific distribution (e.g., normality) for the data and is suitable for comparing two independent samples of per-prompt scores. For each comparison between two methods (Group 1 and Group 2, as detailed in Table 11), we tested the alternative hypothesis ( $H_A$ ) that the scores from Group 1 are stochastically greater than those from Group 2. The detailed results of these tests, including  $p$ -values and findings, are presented in Table 11. Note that statistical tests for FID scores were not performed due to the high computational cost associated with generating multiple full sets of images for each condition required for robust FID variance estimation. FID scores are reported as single values based on one comprehensive generation run per method.

#### C.5 Discussion of diversity, alignment, and fidelity results

The statistical analyses presented in Table 11, along with reported FID scores, provide insights into FairT2I’s performance in terms of image diversity, text-image alignment, and image fidelity, relative to baseline Stable Diffusion models with varying classifier-free guidance (CFG) scales.

**Diversity (Trace Scores).** FairT2I (itself using a CFG scale of 4.0) demonstrates a statistically significant increase in diversity, as measured by both BLIP2 Trace and CLIP Trace, when compared to the original Stable Diffusion model using higher or equivalent CFG scales (i.e., CFG 7.0 and CFG 4.0). Specifically, for both trace metrics, FairT2I’s scores were significantly higher (all  $p < 0.00001$ , except for BLIP2 Trace vs. Original CFG 4.0 where  $p = 0.000002$ ). When compared to the original model with a very low CFG scale (CFG 1.0), which typically yields high diversity, the results are nuanced. While the original CFG 1.0 model achieved numerically higher mean trace scores for both BLIP2 Trace and CLIP Trace compared to FairT2I, these differences were not found to be statistically significant (BLIP2 Trace  $p = 0.255$ ; CLIP Trace  $p = 0.069$  when testing  $H_A$ : Original CFG 1.0  $>$  FairT2I). This suggests FairT2I achieves a level of diversity that is statistically comparable to that of the highly diverse CFG 1.0 setting.

**Text-image alignment (CLIP Score).** For CLIP Scores, the original model with CFG scales of 7.0 and 4.0 yielded statistically significantly higher scores than FairT2I ( $p = 0.021$  and  $p = 0.008$ , respectively, when testing  $H_A$ : Original  $>$  FairT2I). This indicates a slight, yet statistically significant, decrease in text-image alignment for FairT2I when compared to these higher CFG scale baselines. However, when comparing FairT2I to the original model with CFG 1.0, there was no statistically significant evidence that Original CFG 1.0’s CLIP Score was higher than FairT2I’s ( $p = 0.664$ ).

Numerically, FairT2I’s mean CLIP Score was slightly higher than that of Original CFG 1.0. This suggests a trade-off: increasing diversity via FairT2I might involve a small compromise in text-image alignment relative to high-guidance settings, but the alignment remains competitive, especially when compared to other high-diversity configurations like CFG 1.0.

**Image Fidelity (FID) and overall balance.** While statistical tests were not performed for FID due to computational expense, the reported scores (Original CFG 7.0: 27.13, Original CFG 4.0: 26.46, Original CFG 1.0: 34.47, FairT2I: 26.24) indicate that FairT2I achieves the best image fidelity (lowest FID score). It surpasses or matches the fidelity of the original model at CFG 4.0 and 7.0, and is substantially better than the CFG 1.0 setting, which shows a marked degradation in fidelity.

**Conclusion on trade-offs.** Taken together, FairT2I appears to offer a favorable balance. It significantly enhances image diversity over standard CFG settings (4.0 and 7.0) and achieves diversity levels statistically comparable to the very low CFG 1.0 setting. While there is a statistically significant, albeit modest, reduction in CLIPScore compared to using CFG 4.0 and 7.0 with the original model, FairT2I maintains excellent image fidelity (best FID). This presents a notable advantage over simply lowering the CFG scale to 1.0 with the original model, which boosts diversity but at a considerable cost to image fidelity and without a clear advantage in text-image alignment over FairT2I. Therefore, FairT2I effectively increases diversity while largely preserving image quality and maintaining a competitive level of text-image alignment.

Table 11: Statistical comparison of FairT2I with Original Stable Diffusion (various CFG scales) using one-sided Mann-Whitney U tests. For all comparisons, the alternative hypothesis ( $H_A$ ) tested is that the median score of **Group 1** is stochastically greater than that of **Group 2**. Significance level  $\alpha = 0.05$ .

| Metric      | Group 1 | Group 2 | $p$ -value | Finding                          |
|-------------|---------|---------|------------|----------------------------------|
| BLIP2 Trace | FairT2I | CFG 7.0 | <0.000001  | Group 1 significantly higher     |
|             | FairT2I | CFG 4.0 | 0.000002   | Group 1 significantly higher     |
|             | CFG 1.0 | CFG 4.0 | 0.255153   | Group 1 not significantly higher |
| CLIP Trace  | FairT2I | CFG 7.0 | <0.000001  | Group 1 significantly higher     |
|             | FairT2I | CFG 4.0 | <0.000001  | Group 1 significantly higher     |
|             | CFG 1.0 | CFG 4.0 | 0.068690   | Group 1 not significantly higher |
| CLIP Score  | CFG 7.0 | FairT2I | 0.020644   | Group 1 significantly higher     |
|             | CFG 4.0 | FairT2I | 0.008392   | Group 1 significantly higher     |
|             | CFG 1.0 | FairT2I | 0.664210   | Group 1 not significantly higher |

## C.6 Visual Results

This section presents additional visual comparisons for several input text prompts in Parti Prompt dataset. Figures 6 through 9 illustrate images generated using our proposed FairT2I method alongside those generated with classifier-free guidance (CFG) at varying scales (7.0, 4.0, and 1.0). As noted in the captions, a guidance scale of 1.0 effectively corresponds to generation without the influence of classifier-free guidance. Our FairT2I method demonstrates an enhanced capability to diversify generation results, particularly for prompts that do not necessarily involve humans—spanning categories such as animals (Figures 6 and 9), objects (Figure 7), and abstract concepts (Figure 8). Each figure allows for a qualitative assessment of the different generation conditions for its respective prompt.



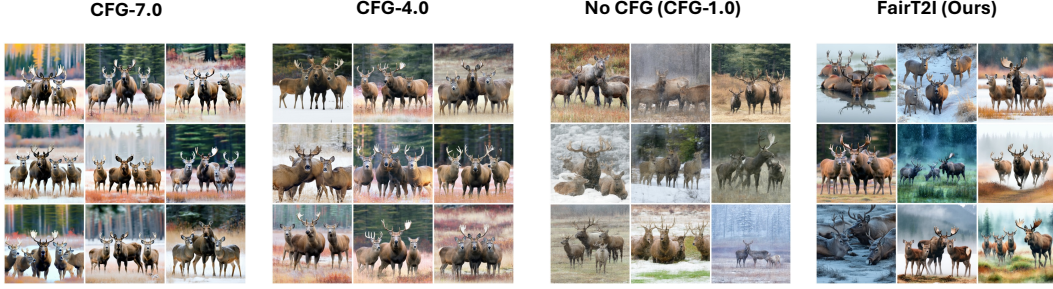


Figure 6: Generated images for the input text “Four deer surrounding a moose.” by classifier-free guidance (CFG) at guidance scales 7.0, 4.0, and 1.0 and FairT2I (Ours). A guidance scale of 1.0 corresponds to generation without CFG.



Figure 7: Generated images for the input text “a Ferrari Testarossa in front of the Kremlin” by classifier-free guidance (CFG) at guidance scales 7.0, 4.0, and 1.0 and FairT2I (Ours). A guidance scale of 1.0 corresponds to generation without CFG.



Figure 8: Generated images for the input text “meaning of life” by classifier-free guidance (CFG) at guidance scales 7.0, 4.0, and 1.0 and FairT2I (Ours). A guidance scale of 1.0 corresponds to generation without CFG.

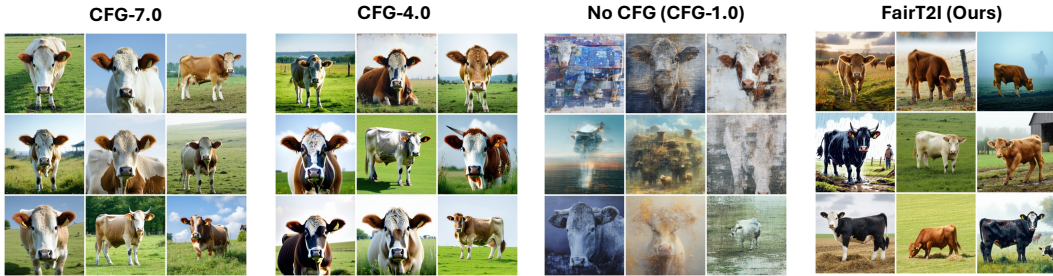


Figure 9: Generated images for the input text “a cow” by classifier-free guidance (CFG) at guidance scales 7.0, 4.0, and 1.0 and FairT2I (Ours). A guidance scale of 1.0 corresponds to generation without CFG.